International Journal of Bioprinting

REVIEW ARTICLE

The application and prospects of 3D printable microgel in biomedical science and engineering

Chengcheng Du[1,2], Wei Huang[1,2]*, Yiting Lei[1,2]*

[1]Department of Orthopedic Surgery, The First Affiliated Hospital of Chongqing Medical University, Chongqing 400016, China

[2]Orthopedic Laboratory of Chongqing Medical University, Chongqing 400016, China

(This article belongs to the *Special Issue: Advances in Bioprinting for Medical Applications*)

Abstract

Three-dimensional (3D) bioprinting technology is one of the most advanced techniques currently applied in tissue engineering and regenerative medicine and has developed rapidly in the past few years. Despite many breakthroughs, there are still several challenges of 3D bioprinting technology awaiting to be addressed, and one of them is the urgency of optimizing bioinks (natural or synthetic hydrogel), which are critical elements in 3D bioprinting, for specific properties. Different from traditional hydrogels, microgels, which are a new type of bioink, are micron-sized gels with excellent mechanical and biological properties, which make them great candidates for applications in 3D bioprinting. Different from the dense and limited pore size of traditional hydrogels, the pore structure of microgel is adjustable, enabling better cell loading before 3D bioprinting, and the printed pores are conducive to the exchange of metabolic substances and cell migration. The "bottom-up" modular microgel has stronger customizable characteristics, and it can freely adjust its mechanical properties, such as hardness, toughness, and rheological properties. In this review, we review the application of microgels in the field of biomedicine and discuss the future development of microgels in 3D bioprinting.

Keywords: 3D bioprinting; Microgel; Bioink; Tissue engineering

***Corresponding authors:**
Wei Huang
(huangw511@163.com)

Yiting Lei
(leiyit614@163.com)

Citation: Du C, Huang W, Lei Y, 2023, The application and prospects of 3D printable microgel in biomedical science and engineering. *Int J Bioprint,* 9(5): 753.
https://doi.org/10.18063/ijb.753

Received: January 18, 2023
Accepted: March 13, 2023
Published Online: May 16, 2023

1. Introduction

Tissue engineering and regenerative medicine address tissue loss issues arising from disease or injury, and three-dimensional (3D) bioprinting has manifested a huge potential in addressing this issue in recent years[1,2]. 3D bioprinting is a technique conducted by coding machines with the ideal goal of reproducibly manufacturing high-precision, biologically active customized tissue or organ structures[3,4]. So far, various 3D bioprinting strategies have been developed to achieve this goal, including stereolithography, inkjet bioprinting, laser-assisted bioprinting, extrusion-based bioprinting, and electrospinning-based bioprinting[5-9]. Different 3D bioprinting strategies have their own advantages and disadvantages[10]. For example, the stereolithographic printing strategy is able to reduce shear forces applied on cells during high-resolution (1 μm) bioprinting, thus ensuring cell viability. However, using this strategy, light is difficult to uniformly pass through the material, leading to uneven crosslinking[6,11].Inkjet printing strategy is relatively low-cost, but it can only produce constructs with a lower cell density, and the printable bioinks that

can be used for this strategy have a limited range of viscosity (3.5–12 mPa·s)[5,6,12]. Laser-assisted bioprinting strategy allows for the application of bioinks with a wider range of viscosity (1–300 mPa·s) and can print products with high resolution and high cell viability. However, this technology is relatively immature and costly[7,13-15]. Electrospinning strategy allows for continuous or discontinuous 3D bioprinting, but fails to print products evenly owing to the charged jet stream[8,16-18]. Compared to the above 3D bioprinting strategies, extrusion-based printing strategy has several advantages: (i) it can print using bioinks with a wider range of viscosity (30 mPa·s to >6 × 10^7 mPa·s); (ii) it can produce constructs with higher cell density (>10^8 cells/mL to cell spheroids); (iii) it can continuously extrude bioinks (making it easier to build products with good integrity); and (iv) it has a relatively simple instrument system that is easy to operate. However, extrusion-based printing is limited by its slow printing speed and extrusion that causes a reduced cell viability[9,10,19-21].

Bioink is one of the most important factors in achieving successful 3D bioprinting, as it almost determines the effectiveness of 3D bioprinting in constructing engineered tissues and organs[22,23]. For 3D bioprinting, bioink needs to possess both mechanical and biological properties. These ensure that the bioink can print stable, intact 3D structures while ensuring that the printed structures can support cell adhesion and proliferation[24]. Gel-based bioinks are the most widely used materials in 3D bioprinting. Currently, there are various gel-based bioinks used in 3D bioprinting, including alginate, fibrinogen, gelatin, collagen, chitosan, hyaluronic acid, methacrylated gelatin (GelMA), polyethylene glycol (PEG) and decellularized extracellular matrix (dECM)[10,23,25,26]. Both natural and synthetic single-component gels have certain limitations. Traditional hydrogels are crosslinked to form a continuous volume (bulk hydrogel), with external dimensions equal to or greater than millimeter scale, and internal pores at the nanometer scale. As a result, the limitations of traditional hydrogels as bioinks mainly lie in their inferior printing resolution and cell culture activity compared to microgel. The size of microgel is in the micrometer range, which is conducive for injection or printing and enable printing of smaller constructs. Moreover, the internal pores or gaps within microgel are also in the micrometer range, which is favorable for cell growth and biological behavior such as proliferation, differentiation, and migration. Additionally, the unique rheological properties of microgel can protect encapsulated cells from shear forces during the printing process[10,22,27,28]. On the other hand, the heterogeneity of microgels enables it to realize multi-layered and multi-component 3D structures in a single print. Microgels can also act as rigid hydrogel networks and form reciprocal networks with single-component hydrogels to enhance the various properties of single-component hydrogels.

In order to address the shortcomings of gels as bioinks, many efforts have been made to improve gels by adding nanoparticles or using multi-component gels as bioinks. While this has resulted in improved properties in the printed products, these bioinks are still not widely used in 3D bioprinting due to their complex design and poor generalizability[25,29-31].

In order to address the challenges of traditional hydrogels as bioink in 3D bioprinting, many researchers have turned their attention to a new emerging bioink called microgel. Microgels are water-based microgels with diameters in the micrometer range that are assembled in a manner similar to hydrogels through processes such as dense packing or jamming. Because the physical interactions between particles are weaker than the covalent bond interactions within particles, microgel can still yield to flow when external forces overcome interparticle friction during printing, while the physical interactions between particles are restored after printing, allowing the printed structure to maintain integrity. Thanks to the covalent bond interactions within the particles, microgels remain intact throughout the process and protect encapsulated cells from damage caused by high shear stresses, further improving the stability of 3D bioprinting[32,33]. Microgels have been reported to be compatible with a variety of material formulations, including hyaluronic acid, agarose, PEG, chitosan, and gelatin. Additionally, their mechanical properties and stretchability can be improved through secondary crosslinking strategies[33].

Due to their unique dynamic structure, excellent biocompatibility, and adjustable mechanical properties, microgels are emerging as a new star player in the field of 3D bioprinting and have a huge potential in the biomedical field. In this review, we briefly introduce the characteristics and preparation strategies of microgel. Then, we focus on the use of microgels to construct 3D objects in the biomedical field. Finally, we summarize the challenges faced and discuss how to further utilize these microgels for 3D bioprinting.

2. Strategies for preparing microgels

Hydrogels possess high water content and characteristics similar to extracellular matrix, which are the attributes leading to their widespread use in the field of 3D bioprinting. Hydrogels form polymer networks through physical or chemical crosslinking, with internal pore sizes at the nanoscale level. This limits their biocompatibility as a bioink and hinders cell adhesion, migration, and

Table 1. Comparison of different strategies used to manufacture hydrogel particles

Preparation strategies for HMPs	Particle geometry	Minimum size range	Particle size coefficient of variation	Productivity
Batch emulsion	Spherical	1–10 μm[161]	>10%[37]	High
Microfluidic technique	Spherical	5–10 μm[162,163]	<2%[40]	Moderate
Photolithography	Controllable geometry	<1 μm[164]	<3%[165]	Low
Electrostatic spraying	Spherical	1–10 μm[166]	>50%[167]	Moderate
Mechanical crushing	Irregular shape	>20 μm[56]	>5%[57]	High

proliferation[34-36]. In an alternative strategy, hydrogels can be fabricated into microspheres of various micron sizes, known as microgels. Generally, the strategies for preparing microgels are classified into batch emulsion, microfluidic technique, photolithography, electrostatic spraying, and mechanical crushing (Table 1).

2.1. Batch emulsion

The batch emulsion method utilizes an immiscible oil and water gel precursor solution to produce microgel. The basic process involves the mixing of a water gel solution (containing an initiator) with oil in a container, and the mixture is mechanically stirred to homogenize the solution and ultimately produce microgel encapsulated by the oil phase. The degree of mixing, duration, and intensity of mechanical force all influence the particle size and dispersion of the microgels. Following the production of the microgels, crosslinking is typically performed through the use of photopolymerization, after which the oil phase is removed through steps such as washing, centrifugation, and filtration to obtain usable microgels. Overall, this microgel production method is simple and efficient, with a high production rate. However, some of its drawbacks are the microgels produced having a particle size coefficient of variation >10%[37] and the poor dispersion, which can be improved by continuous filtration of a highly disperse microgel suspension through a filter, as proposed by Truong *et al.*, to obtain more monodisperse suspensions[38].

2.2. Microfluidic technique

Microfluidic technique involves guiding the flow of oil and water phases at a cross junction to achieve controlled formation of microgels. Shear force and hydrophobic interactions induce the formation of water droplets within the oil phase[27]. By changing the geometric shape of the intersection and the relative velocities between the two phases, the diameter of microgels (5–500 μm) can be controlled[39]. By maintaining stable relative velocities, highly monodisperse microgel suspensions with excellent dispersity indices (1%–2%) can be obtained[40]. One limitation of the microfluidic technique is the low production rate. To address this issue, Kamperman *et al.* developed an air microfluidic strategy in which two microscale liquid flows are sprayed together and collide, ultimately forming microgels with a production rate that is 10–100 times faster than the traditional microfluidic strategies[41]. In addition to air-based microfluidic strategies, the use of multi-array high-throughput microfluidic chips is also an effective approach to improve the production rate of microgels[42]. For example, Chung *et al.* developed a multi-layer integrated microfluidic droplet generator that can produce a large quantity of highly uniform microgels[43]. This strategy allows for precise control of the number of cells in each microgel, even down to the single-cell level, by controlling process parameters such as the particle size and density of cells in the precursor solution. Additionally, high-throughput generation of cell-laden microgels can be achieved through parallelized channels[44,45]. Furthermore, high-throughput centrifugal microfluidic technique is another emerging method for mass-producing hydrogel microspheres[46,47]. The centrifugal microfluidic device can be easily assembled onto a conventional centrifuge, demonstrating high scalability and suitability for large-scale production of hydrogel microspheres[48].

2.3. Photolithography

Photolithography techniques can be broadly categorized into three types: imprint lithography, photolithography, and flow lithography. In the imprint lithography strategy, a hydrogel precursor is loaded into a mold with the desired microgel characteristics, and crosslinked, followed by solidification[49]. In the photolithography process, the precursor solution of hydrogel is selectively solidified by templated photomasks, ultimately resulting in the formation of microgel[50]. In the case of flow photolithography, the precursor solution of the flowing hydrogel is periodically solidified by a light mask, ultimately resulting in the formation of microgel[51]. The advantage of the photolithography method lies in its ability to precisely control the geometric shape and monodispersity of the microgel, but it is limited by the mold and has low yield. Currently, several methods have been developed to increase the yield of microgel produced through photolithography techniques, such as accelerating the curing rate of the hydrogel precursor, enhancing the intensity of the light source, or increasing the concentration of initiators[52,53].

2.4. Electrospray

The basic principle of the electrospray method is to establish an electric field between the metal needle and the receiving device, which enables the droplets to overcome the surface tension and be sprayed into the receiving device. After crosslinking, microgels are formed. The particle size of the microgels depends on the applied voltage, needle diameter, and flow rate[54]. This method can produce microgels with extremely small diameter (as small as 1 μm), but the dispersion of hydrogel microparticle suspensions is poor[55]. The electrospray method is less commonly used in the production of microgels.

2.5. Mechanical fragmentation

Mechanical fragmentation is a method of breaking down already formed hydrogel into microgel through physical means, such as using a fine wire mesh for forced mechanical fragmentation of the hydrogel[56], or using a rotary stirrer to break down crosslinked hydrogel into hydrogel–microgel[57]. Mechanical fragmentation has an extremely high yield of microgel, but it is unable to accurately control the shape and size of microgel[27]. In 3D bioprinting, the batch emulsification and mechanical fragmentation methods are widely used due to their simplicity and fast production speed.

3. Strategies for assembling microgels

To prepare for 3D bioprinting, it is necessary to process the obtained microgel into printable microgel. The self-assembly of these microgels can be facilitated through interparticle interactions, and the assembly strategies can be categorized based on the strength of these interactions. This classification system allows for a more efficient and targeted approach to the self-assembly process, thereby improving the overall success of the 3D bioprinting process. The advantages and disadvantages of the microgel assembly strategy are summarized in Table 2.

3.1. Gravity

Gravity packing is the most commonly used method to "jam" the microgel as a bioink (Figure 1A)[28]. In the "jammed" state, the particles within the microgel move as a cohesive whole, resulting in the material behaving as a solid at the macroscopic level until sufficient force is applied to cause movement[27,58,59]. The mechanism behind this occurrence is that as the concentration of microgel increases, the interparticle friction also increases, leading to deformation of the microgel under external force. It is typically observed that a transition from hydrogel particle blockage occurs when the volume fraction of the microgel reaches approximately 0.58[32]. The jamming of microgel is mainly influenced by frictional forces, and the van der Waals forces between adjacent microgels are negligible. As a result, jammed microgels exhibit viscous fluid-like behavior under shear stress and recover to a viscoelastic solid upon release of external load. When the particle volume fraction of microgel is between 0.58 and 0.74, jammed microgel display excellent shear thinning and self-healing properties[60]. The flow and recovery properties of this responsive pressure approach fulfill the design requirements for 3D bioprinting ink, allowing for the theoretical possibility of printing microgels with any constituent composition based on this strategy[61].

Through the process of gravity packing, Highley *et al.* prepared a microgel (NorHA) using norbornene-modified hyaluronic acid, PEGDA, and agarose[61]. The NorHA microgel was prepared using a microfluidic device and had a diameter of approximately 100 μm. It exhibited good rheological properties upon jamming, with its viscosity decreasing with increasing shear rate and shear yield increasing with strain. It also displayed the ability to flow during extrusion and rapidly stabilize upon sedimentation (Figure 1B–D). NorHA microgel can be printed layer by layer through the use of an extruder, resulting in structures with short-term stability. Through post-printing photopolymerization, the compressive modulus of the printed structures is further enhanced, allowing for long-term stability. In addition to layer-by-layer printing, these microgels can also be used as bioinks for 3D-printing solid structures. One of the most important evaluation criteria for bioinks used in 3D bioprinting is the viability of encapsulated cells, and NorHA microgels have been shown to maintain cell viability at around 70% after encapsulation prior to printing[61].

3.2. Chemical effect

The assembly of microgels can be induced through chemical interactions, including enzyme catalysis, photopolymerization, click chemistry, and amine coupling reactions (Figure 2A), which typically involve the irreversible formation of covalent bonds[62].

Enzyme catalysis refers to a chemical reaction that is catalyzed by an enzyme[63]. Currently, the enzymes reported to be used in microgel assembly are primarily transglutaminases. Song *et al.* developed a microgel mediated by transglutaminase, which is composed of a discrete phase (enzyme-crosslinked gelatin microgel) and a crosslinkable continuous gelatin precursor solution containing transglutaminase. This microgel has good injectability and cell loading activity[64]. The enzyme-mediated microgel assembly process is typically carried out under mild conditions (neutral pH and moderate temperature), allowing for the incorporation of live cells into dynamically formed microgel assemblies[28].

Table 2. Advantages and limitations of microgel assembly strategy

Assembly strategy	Advantages	Limitations
Gravity	• Mild reaction conditions • Simple and feasible • A wide range of applications	• Weak binding, usually requires secondary crosslinking • Difficult to achieve high-precision 3D printing
Enzyme catalysis	• Mild reaction conditions • Excellent cytocompatibility	• Unstable enzyme activity • The involvement of enzymes may trigger side reactions
Photopolymerization	• Mild reaction conditions • Short reaction time	• Possible damage to cells caused by the released active free radicals • Microgels are susceptible to incomplete crosslinking within
Click chemistry	• Mild reaction conditions • Efficient and fast	• Complex chemical modification process
Amine coupling reactions	• No additional modification process • Faster assembly	• Crosslinking agents may react with proteins and thus damage cells
Host–guest interaction	• Good biocompatibility • Rapid self-assembly • Non-toxic crosslinker	• Complex functional group modifications required • Weak and unstable binding force, especially in aqueous solutions
Electrostatic interaction	• Fast assembly process • Non-toxic crosslinker • Good biocompatibility	• Electrostatic interactions are easily disrupted, especially in electrolyte solutions
Hydrogen bonding	• Good biocompatibility • Adjustable bond strength • Non-toxic crosslinker	• Complex and costly method to enhance hydrogen bond strength
Biotin and streptavidin conjugation	• Good biocompatibility • Rapid self-assembly • Stable interaction	• Irreversible interaction
Cell–cell junction	• Good biocompatibility • Non-toxic crosslinker • Allows construction of 3D tissues with uniform cell density	• Assembly process is relatively slow and depends on the cell's own ability
Fluid forces	• Precise one- or two-dimensional structures • Fast assembly	• Assembled product is not stable • Difficult to build 3D structure products
Surface tension	• Good biocompatibility • Fast assembly • Compatible with most microgels	• Unable to precisely control product size • Requires secondary crosslinking to stabilize assembly • Difficult to build 3D structure products
Magnetic forces and acoustic forces	• Fast assembly • Compatible with most microgels	• Potential cytotoxicity of magnetic nanoparticles

The initiation of free radical polymerization by light involves the decomposition of initiators under light exposure, generating free radicals that trigger continuous polymerization reactions[65]. Sheikhi *et al.* prepared GelMA hydrogel–microgel using microfluidic technology, and these microgel formed a network connection through low temperature-induced physical crosslinking. Subsequently, photogenerated free radical polymerization was used to fabricate a highly mechanically elastic 3D GelMA scaffold[65]. In summary, photogenerated free radical polymerization requires mild reaction conditions (usually at room temperature) and relatively short reaction times.

Click chemistry is a highly selective and efficient chemical reaction that involves the formation of carbon-heteroatom bonds (C-X-C) to link molecules together. This type of reaction can be utilized to assemble various microgel[59,66]. Xin *et al.* prepared PEG microgel via a non-chemical metathesis method using thiol-ene click chemistry[67]. These PEG microgels have highly adjustable physical and chemical properties, while also maintaining long-term stability of the printed structure[67].The assembly process of click chemistry-based microgel is fast and mild, resulting in a final product with good cell compatibility. However, the assembly strategy often involves complex functional group modification and synthesis steps.

Microgels containing peptides or proteins can be assembled through a cyanylation reaction, in which the hydrogen atoms on the amino group are replaced by cyanyl groups[68].Generally, this type of reaction does not require additional modification processes and has a

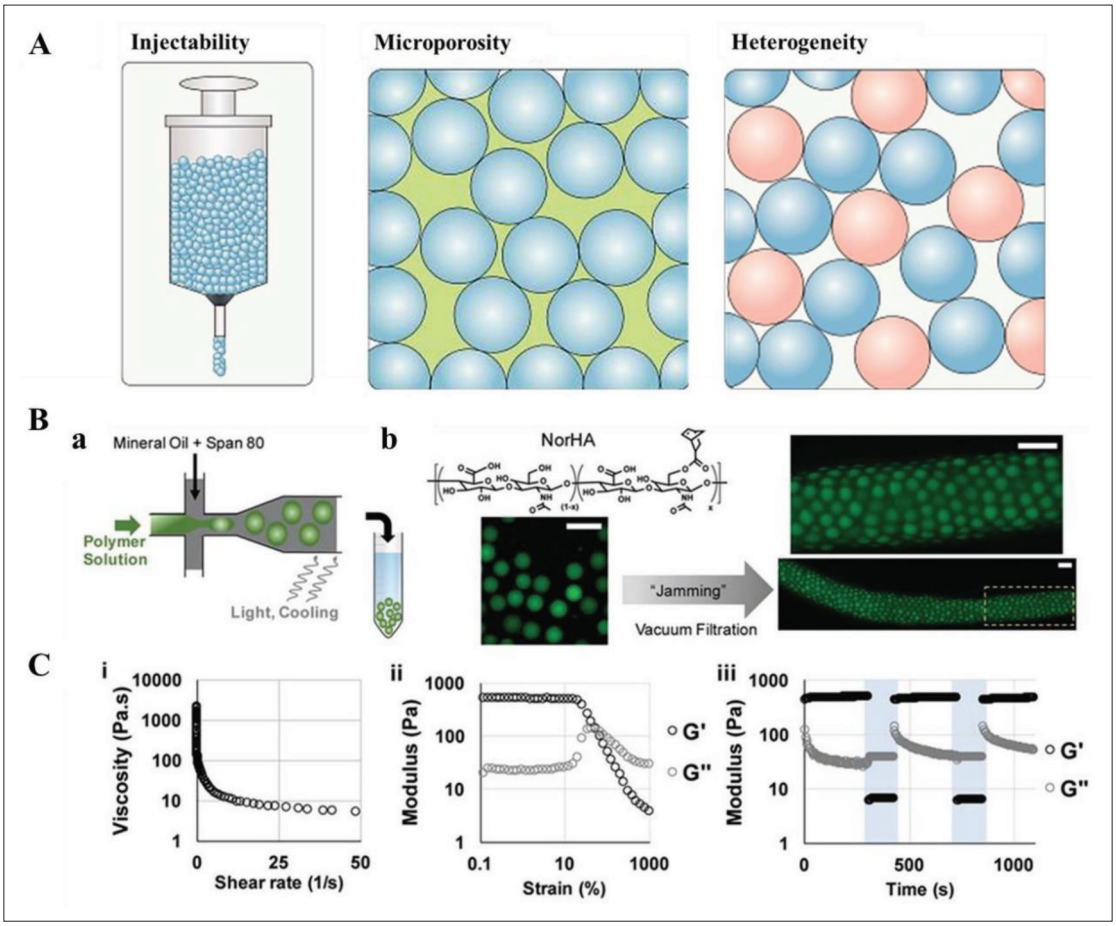

Figure 1. Gravity-assembled microgels. (A) Microgels have unique features, including injectability, heterogeneity, and porosity, which allow for passage through the structure. Interlinking between particles further stabilizes the structure. [from ref.[28] licensed under Attribution-NonCommercial-NoDerivatives 4.0 International (CC BY-NC-ND 4.0)]. (B) Jammed microgel ink fabrication, rheological properties, and extrusion. (a) The process of microfluidic preparation of microgels. (b) Representative fluorescent images of suspended microgels (left) fabricated from 2 wt% NorHA that are jammed through vacuum filtration into a solid (right) that can be extruded from a syringe. (C) Rheological characterization of jammed NorHA microgel inks showing (i) decreased viscosity with continuously increasing shear rates (0–50 s^{-1}), (ii) shear-yielding with increase in strain (0.037%–1000%, 1 Hz), and (iii) shear-thinning and self-healing through low (unshaded, 1% strain, 1 Hz) and high (shaded, 500% strain, 1 Hz) strain cycles. [(from ref.[61] licensed under Creative Commons Attribution 4.0 license)].

relatively fast reaction rate, and the resulting microgel have good biocompatibility. For example, Li *et al.* used N-hydroxycarbamyl-amine coupling to assemble water-based micromicrogel containing human bone marrow mesenchymal stem cells (MSCs). In this crosslinking process, the microgel also had the potential to rapidly bond with tissue models, which could be useful in the implementation of in situ printing[68].

3.3. Physical effect

Through physical interactions between microgels, typically non-covalent interactions, the assembly of water-based microgels can be achieved (Figure 2B). Common physical interactions include host–guest interactions, electrostatic interactions, hydrogen bonding, and biotin-streptavidin conjugation[69]. Microgels formed through physical action have typically been found to possess self-healing, shear thinning, and injectability, but tend to have lower mechanical strength compared to those assembled through chemical action.

The self-assembly of microgel through host–guest interactions refers to the formation of specific polymers through the self-assembly of monomer molecules based on the recognition characteristics between the host and guest[70]. For example, by using cyclodextrin as the host and adamantyl as the guest in the self-assembly of microgels, different microgels can be selectively assembled by altering the size and shape of the host and guest components. Overall, the assembly of microgels through the interaction between main and secondary objects occurs at a fast rate, resulting in microgels with strong biological compatibility.

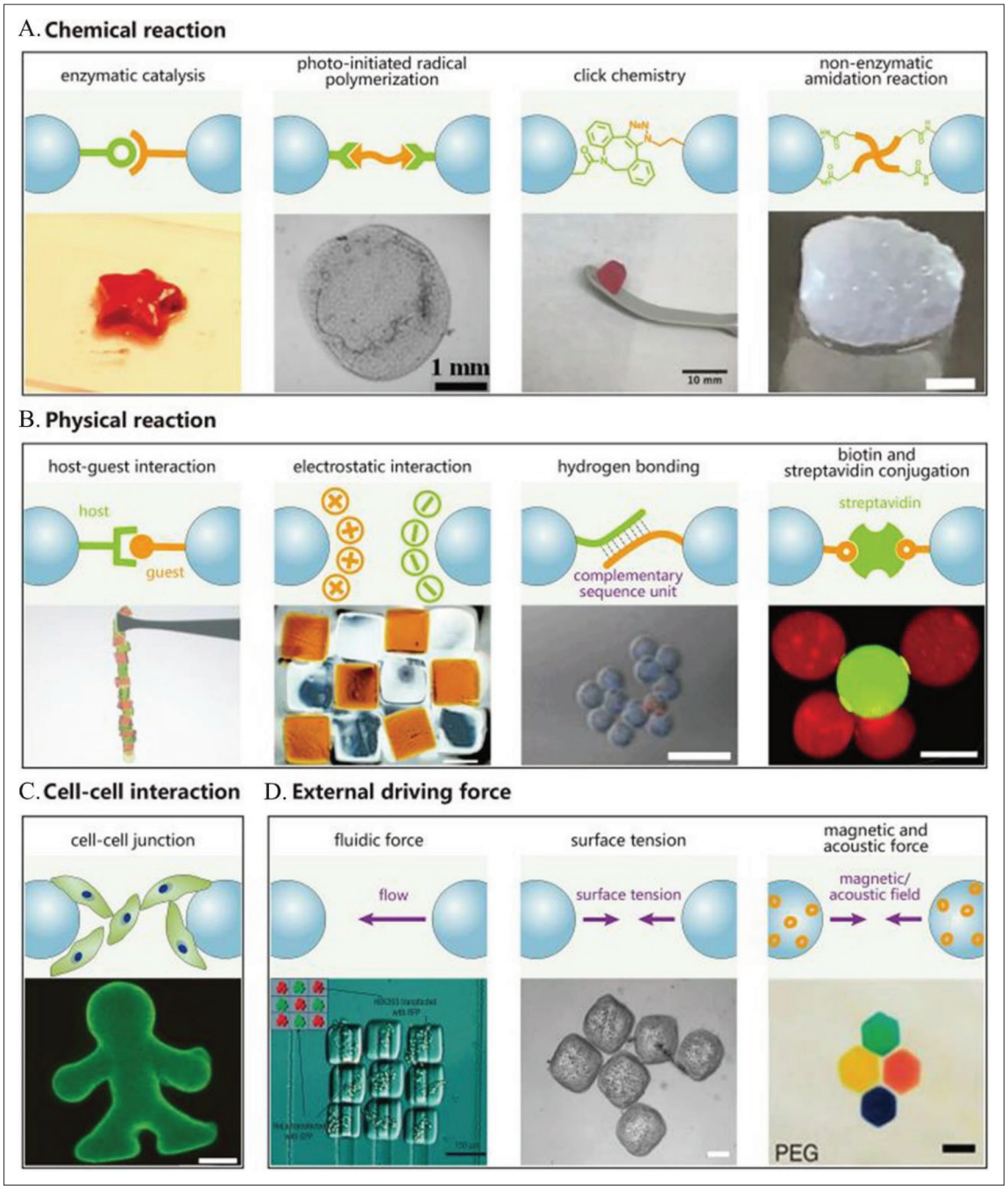

Figure 2. Strategies for assembling microgel. (A) Chemical reaction. (B) Physical reaction. (C) Cell–cell interaction. (D) External driving force. [(from ref.[28] licensed under Attribution-NonCommercial-NoDerivatives 4.0 International (CC BY-NC-ND 4.0)].

However, these microgels often require complex functional group modifications and have weak and unstable binding abilities.

Electrostatic forces can serve as a driving force in the assembly process of microgels, allowing for the convenient, rapid, and mild condition-based assembly of microgels through electrostatic interactions. For example, Xu *et al.* used photo-crosslinked GelMA and chitosan low polymer-methacrylate (ChitoMA) as negatively and positively charged building blocks, respectively, to assemble microgels that can spontaneously form interconnected pores with good cell compatibility[71,72]. The assembly of microgels through electrostatic interactions is rapid

and easy, but due to the lack of strong charges between the assembled microgels, this interaction is weakened in electrolyte solutions.

The assembly of microgels can also be achieved through the interaction of multiple hydrogen bonds, although the effect of individual hydrogen bonds is relatively weak. However, the microgels formed by the action of a large number of hydrogen bonds have high mechanical strength. For example, the number of hydrogen bonds in the microgels that are made by mixing chitosan methyl acrylate and polyvinyl alcohol (PVA) after repeated freezing and thawing increase, thereby greatly enhancing its mechanical strength[36,73].

The biomolecule-chain melanin affinity interaction is one of the strongest non-covalent interactions. The microgels assembled through this interaction are extremely stable, but at the same time, this binding interaction is irreversible. Hu *et al.* used microfluidic technology to prepare biomolecule-functionalized alginate microgel. By incubating the biomolecule-functionalized microgel with soluble chain melanin affinity protein for a short period of time (about 5 min), microgels can be assembled[74].

3.4. Cell–cell junction

Self-assembly of hydrogel–microgel can be achieved through intercellular interactions such as cell–cell or cell–matrix adhesion. In other words, cells are cultured on the surface of hydrogel–microgel, and the binding forces between cells drive the assembly of the hydrogel–microgel (Figure 2C). For example, Matsunaga *et al.* cultivated cells on the surface of single dispersed collagen hydrogel–microgel, and then stacked the cell-coated hydrogel–microgel in a mold to trigger intercellular interactions and assemble it into a hydrogel[75]. This assembly method can reconstruct 3D tissue with uniform cell density[75]. The self-driven forces of cells spontaneously drive the assembly of microgel in this manner, without the involvement of external factors, resulting in excellent biocompatibility of the assembled microgel. However, several challenges are faced in this assembly process, including the requirement for microgels with a certain degree of cell adhesion ability on their surface, and the need for microgels that are conducive to cell proliferation and migration, with sufficient cell growth speed to maintain efficiency in the assembly process.

3.5. External driving force

Common external driving forces for the assembly of microgel include fluid forces, surface tension, magnetic forces, and acoustic forces (Figure 2D). The rapid assembly of microgel can be achieved through the use of external driving forces, but the resulting structures tend to be unstable and prone to structural instability or even collapse upon removal of the external forces[28,76].

Fluidic forces are commonly used to assemble polymer precursors into microgel through the application of external forces on a one- or two-dimensional microfluidic channel device, ultimately resulting in the formation of the microgel at the outlet of the device[77]. This assembly method has the advantage of precise control over the assembly process, allowing for the design of specific shapes for the microgel. Surface tension is utilized in the assembly of microgel, with microgel solutions in an oil or gas phase being closely stacked due to the surface tension at the liquid–liquid or liquid–gas interface, and completed upon the removal of the oil or liquid phase. This method is quick and simple, but the assembled microgels are not stable and the size of the assembled microgels cannot be accurately controlled[78-80].

Under the influence of an external magnetic field, microgels containing magnetic nanomicrogels are capable of assembly, and the assembly of the microgels can be controlled through the design of devices with different shapes and the adjustment of the intensity of the external magnetic field. Currently, there is also a method for assembling 3D-shaped microgels (including multilayer cylindrical and spherical structures). This method is fast in assembling microgels and is able to prepare complex and precise 3D-structured microgels; however, the cytotoxicity of the magnetic nanomicrogels limits their use in tissue engineering[81,82]. Microgels can also be assembled through an external acoustic field, in a way similar to the driving force of a magnetic field. When the suspended microgels are subjected to an external sound wave, they can be assembled into single- or multi-layer structures. However, microgel structures assembled solely through the action of sound waves are typically unstable and require secondary crosslinking for stable structure[83].

4. Characteristics of microgels

4.1. Biological properties of microgels

Bioink is defined as a cellular formulation, potentially containing bioactive components and biomaterials, that is suitable for processing through automated biomanufacturing techniques[84]. In terms of function, an ideal bioink must be able to be printed through bioprinting technology, maintain cellular viability, and trigger the desired cellular response[85,86]. The biological characteristics and biocompatibility of microgels are crucial for the realization of 3D bioprinting[10]. Microgels must be able to maintain the health and vitality of cells during the process of bioprinting, and protect cells during the process of bioprinting. For ordinary hydrogels, the

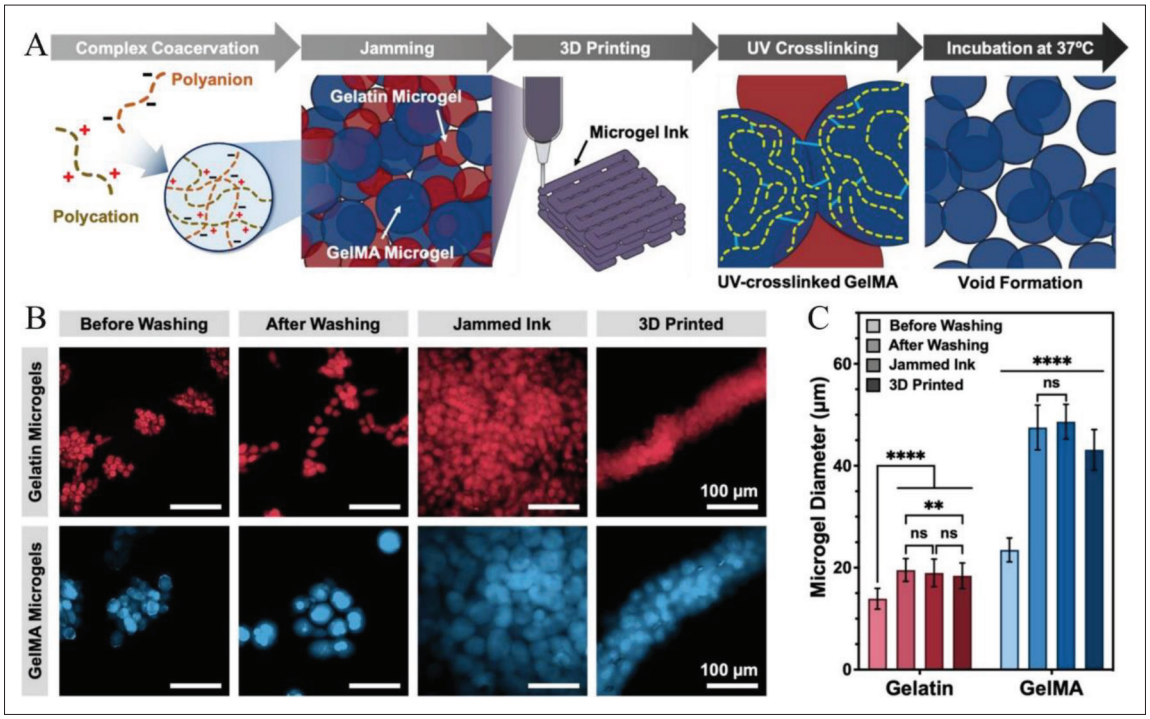

Figure 3. Design of microporous GelMA microgel inks with sacrificial gelatin microgels. (A) Schematic illustration depicting the process for producing 3D-printed constructs with tunable void fraction. (B) False-colored image of a representative sample of rhodamine B-stained gelatin and GelMA microgels before washing, after washing, after jamming, and after 3D printing. (C) Particle diameter of GelMA and gelatin at each stage. Reprinted with permission from Seymour, A. J., Shin, S., Heilshorn, S. C., *Adv. Healthcare Mater.* Copyright © 1999-2023 John Wiley & Sons[89].

latter presents a challenge, as the shear forces generated during printing can damage the vitality of cells. However, microgels can effectively address this issue, as cells are able to be encapsulated within hydrogel–microgel or retained within the interstitial spaces between hydrogels and microgels[87,88].

In comparison to hydrogels with nanometer-sized internal pores, cells tend to disseminate more quickly and extensively within microgel. The interstitial space between microgels typically forms a 3D, interconnected porous network through which cells can freely migrate and exchange biological information[88]. The size of the internal pore structure of microgel is correlated with the diameter size of the hydrogel–microgel, with micrometer-sized microgel generating micrometer-sized pores. Given that most cells are at the micrometer scale, microgels possess excellent biocompatibility. Seymour *et al.* demonstrated a strategy for controlling the size of the interstitial space in microgel by mixing gelatin microgel with GelMA in 3D bioprinting to control the total porosity of the microgel (Figure 3A and B)[89]. The average particle size of the gelatin and GelMA hydrogels obtained through bulk emulsification method were 18.0 ± 3.97 μm and 50.55 ± 14.31 μm, respectively. The GelMA hydrogel displayed a more uniform spherical shape (aspect ratio of 1.16 ± 0.12), while the gelatin population exhibited a higher rate of elongated hydrogel formation (aspect ratio of 1.35 ± 0.26). The products of hydrogel printing were immediately crosslinked by ultraviolet light, followed by the removal of the gelatin. The average porosity of the printed products could be adjusted through the ratio of gelatin to GelMA hydrogel, with average porosities ranging from approximately 0.28 ± 0.04 to 0.41 ± 0.02 to 0.57 ± 0.06 when the GelMA:gelatin hydrogel ratio was 80:20 to 60:40 to 40:60, respectively (Figure 3C). Human umbilical vein endothelial cells (HUVECs) exhibited good cellular viability (greater than 95%) in all proportions of microgel, with the highest level of cellular infiltration and migration observed in the 40:60 microgel[89].

Microgels have been shown to not only enhance cellular viability, but also promote biological changes in cells. MSCs encapsulated in a chitosan-derived microgel demonstrated improved differentiation potential toward chondrogenesis, with notable upregulation of chondrogenic genes such as *SOX9*, *Aggrecan*, and *Col2A1* compared to cells in a conventional hydrogel. Additionally, levels of glycosaminoglycan (GAG) expression were significantly increased[68]. Tissue regeneration can be promoted in PEG microgel. In a skin wound healing model, microgel exhibited stronger re-epithelialization

ability than ordinary hydrogels. On the fifth day of using the microgel, hair follicles and sebaceous glands appeared in the wound, almost achieving tissue regeneration[63]. Hyaluronic acid-based microgels have demonstrated the ability to facilitate the migration of neural stem cells toward wounds and the formation of blood vessels, exhibiting good tissue remodeling capabilities. This suggests a potentially significant application in the context of irregular spinal injuries[90]. The modified heparin chitosan microgel were found to effectively repair bone defects in type II diabetes rat models while also improving the immune microenvironment[91]. It has been consistently found in these studies that the unique pore size of micromicrogel plays a crucial role in improving cellular responses.

The most notable biological characteristic of microgels is their microscale pore network, which closely mimics the microenvironment for cell survival. Compared to traditional hydrogels, microgels are more conducive to cellular behaviors such as growth, proliferation, differentiation, and migration. According to extensive research comparisons, the principle behind this may be that the interconnected micropores and void spaces not only facilitate the transport of nutrients, thereby increasing cell vitality, but also promote cell infiltration and vascular formation without having to wait for hydrogel degradation. In addition to the above, microgels also exhibit excellent encapsulation properties, as they can modify the microscale features such as particle size and shape of microgels to adjust the release profile of growth factors or drugs. Meanwhile, microgel heterogeneity allows multiple release profiles and degradation behaviors of growth factors or drugs to be incorporated into a single printing process, which is advantageous for many tissue repair strategies to match the multi-level biological signaling[63,92,93].

4.2. Mechanical properties of microgels

As a bioink, microgel possesses excellent shear viscoelastic capabilities, allowing it to be extruded through a printing head while protecting encapsulated cells from damage due to high shear forces. The elegance of using microgel for 3D printing lies in the smooth transition between the fluid and the solid states[94,95]. This transformation is highly related to the structural characteristics of microgel, which differ from hydrogels in that they are composed of micrometer-sized hydrogel–microgel within their interior. The interaction between these micromicrogels results in the microgel exhibiting solid-like behavior but becoming liquid-like under the influence of external stress. Therefore, the porosity and hardness of the micromicrogel largely determine the mechanical properties of the microgel[60]. When the accumulation fraction of microgel reaches 0.58, the microgel exhibits as solid state. As the accumulation fraction increases, the friction between microgels increases, causing the microgels to become more "solid" in a blocked state. Theoretically, when the accumulation fraction reaches 0.64, single dispersed microgel can reach the maximum blocked state under random configuration. When the accumulation fraction reaches 0.74, perfect accumulation can be achieved. In the state of particle accumulation, the microgel exhibits shear thinning and self-healing characteristics. Studies have reported that tyramine-modified hyaluronic acid microgel (particle diameters of 40, 100, and 500 μm) have similar yield stress (139 Pa). In repeated cycles at low (1%) and high (500%) strain, all bioinks transition from solid ($G' > G''$) to liquid-like ($G'' > G'$) under high shear stress. In low shear mode, all bioinks exhibit excellent shear recovery performance, with the initial storage modulus reaching 100%. There is a significant negative correlation between elastic modulus and pore diameter, with $E = 9.9 \pm 3.6$, 7.5 ± 2.4, and 5.7 ± 2.2 kPa when the pore diameter is 40, 100, and 500 μm, respectively. This microgel exhibits excellent printability, enabling the 3D bioprinting of cells with the ability to strengthen the printed structure through post-print crosslinking (Figure 4B and C)[96]. Microgels are not limited to spherical microgels, as hydrogels with high aspect ratios (hydrogels) can also form microgels. Kessel *et al.* reported a "microchain" microgel based on hyaluronic acid-methyl acrylate (HA-MA), with a microchain diameter of 40–100 μm and a microgel porosity ranging from $7.4 \pm 0.9\%$ to $2.0 \pm 0.8\%$[97]. The yield stress of the microgel changes with the degree of crosslinking and the diameter of the microchain, with higher crosslinking resulting in lower yield stress and larger microchain diameters resulting in higher yield stress. Shear recovery was found to be the best in microgel with moderate crosslinking, at approximately 82%, while the highest crosslinked microgel had a shear recovery of around 70% and the lowest crosslinked microgel had a shear recovery of around 20%. This microgel exhibits good cell loading ability, enabling the loading of cells prior to microgel assembly or post-assembly (Figure 4E)[97].

The mechanical strength of microgel is also a critical factor in achieving 3D bioprinting. After 21 days of printing, the elastic moduli of tyramine-modified hyaluronic acid microgel with pore sizes of 40 μm, 100 μm, and 500 μm were 103.6 ± 18.5, 83.9 ± 19.7, and 78.1 ± 19.2 kPa, respectively, while the elastic modulus of the control group was 58.3 ± 30.2 kPa. After 63 days, the elastic moduli of microgel with pore sizes of 40 μm, 100 μm, and 500 μm were 145.3 ± 22.3, 201.6 ± 8.9, and 152.6 ± 47.2 kPa, respectively, while the elastic modulus of the control group decreased to 33.7 ± 17.2 kPa (Figure 4C)[96]. Yang *et al.* reported on a PAAm/PAMPS microgel based on a resilient particle double network (P-DN) hydrogel, which possesses two

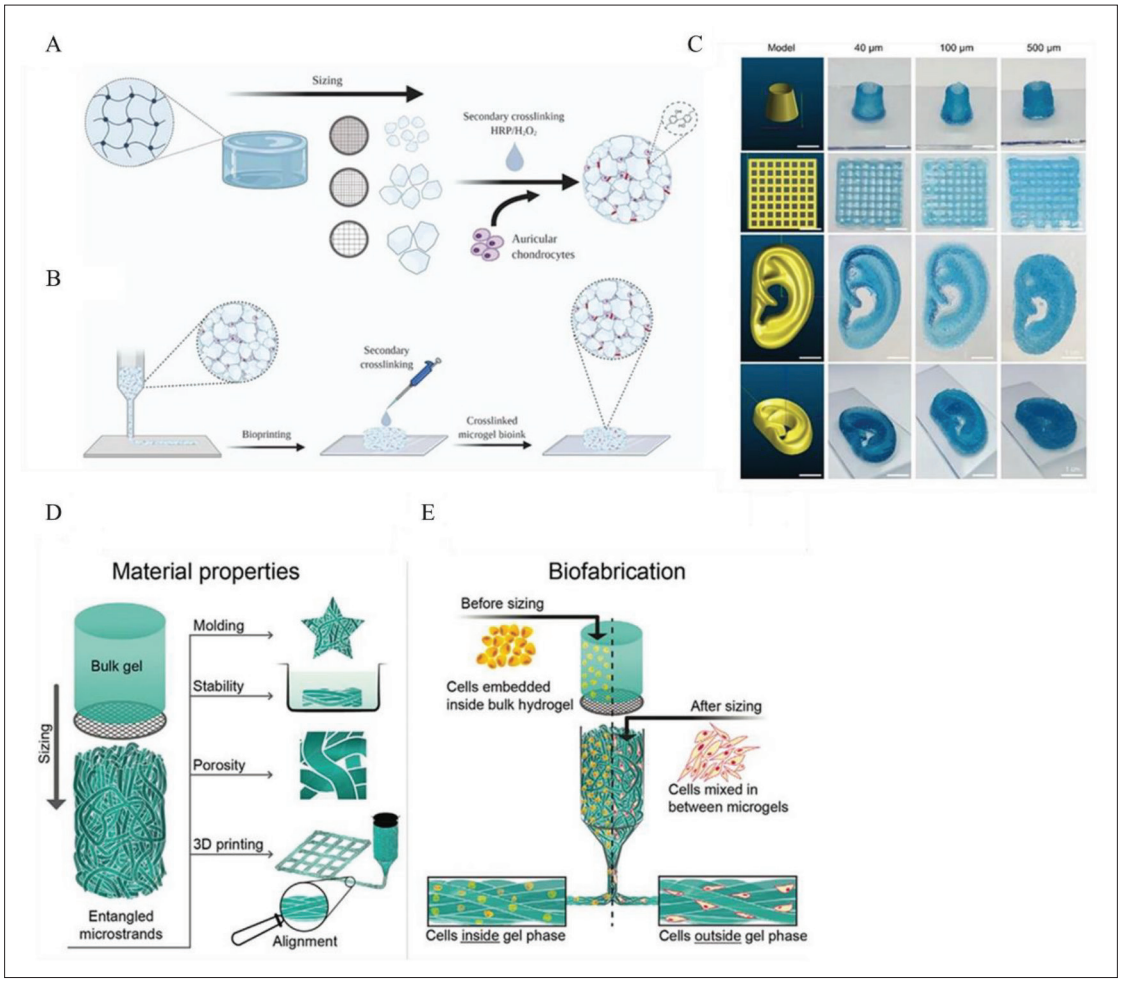

Figure 4. 3D Bioprinting of macroporous materials based on entangled hydrogel microstrands. (A) Sizing of the bulk tyramine-modified hyaluronic acid (HA-TYR) hydrogels using grids with aperture diameter of 40, 100, and 500 μm. (B, C) 3D printing schematic of HA-TYR bioinks. The cell-laden microgels can be printed through a 0.61-mm nozzle and stabilized by secondary crosslinking [(from ref.[96] licensed under Creative Commons Attribution 4.0 license)]. (D) The bulk hydrogel forms a microchain structure after mechanical crushing, and has moldability, stability in aqueous solutions, porosity, printability. (E) A bioink can be created by embedding cells in bulk hydrogel before sizing that results in a spatial deposition of cells inside the gel phase. Alternatively, cells can be mixed in between the already prepared entangled microstrands, so cells occupy the space outside the gel phase [(from ref.[97] licensed under Creative Commons Attribution 4.0 license)].

networks: a solid but brittle microgel network and a soft hydrogel network. As a result, this P-DN microgel exhibits exceptional stretchability. The viscosity, yield stress, and strength of this microgel increase with increasing particle concentration, and its fracture toughness is capable of reaching 3000 J m^{-2}[98]. Seymour *et al.* reported a strategy involving the mixing of two microgels (GelMA: gelatin) and the removal of the gelatin microgel after crosslinking, which resulted in a final microgel with controllable pore size by manipulating the mixing ratio and diameter of the two microgels[89]. According to the experimental results, these microgels showed a decrease in storage modulus as the pore ratio increased, with the highest (pure GelMA microgel) and lowest ratio (40:60) storage moduli being 4.5 ± 1.0 kPa and 177 ± 26 Pa, respectively[89]. It can be seen that the mechanical properties of microgels are sufficient to meet the needs of most 3D bioprinting, while also having strong customizability.

The flow of hydrogel–microgel during the process of 3D bioprinting differs significantly from the liquid flow of ordinary hydrogels. In order to achieve an ideal printing effect, there are still many challenges to be addressed. To address this issue, Xin *et al.* utilized thiol-epoxy PEG microgel as biological ink and studied ways to improve printing performance[67]. They first constructed microgels in three different sizes (single disperse 100 μm, single disperse 150 μm, and multiple disperse 200 μm) for testing and found that single disperse microgel could be easily printed by nozzles with diameters of 200–400 μm, while multiple

disperse microgels required larger nozzles (410–610 μm) to print smoothly. For a monodisperse microgel, smaller nozzle sizes (200 μm) are able to produce 3D structures with higher finesse than larger nozzle sizes (250 μm). In order to study the effect of the stiffness of water-based microgel on the printing process, three microgels (PEG5, PEG10, and PEG20) were constructed, with Young's moduli of 30–40 kPa, 20 kPa, and 10 kPa, respectively. When subjected to the same pressure (15 μN) during the printing process, the PEG20 microgel showed greater deformability. The stacking of cylindrical prints was performed without secondary crosslinking, with stack heights of 20 mm, 10 mm, and 5 mm for the three respective microgels. After the cells were packaged and printed for three days, the viability of cells within the microgel was approximately 90%, 90%, and 40%, respectively. The increased stiffness of hydrogel microspheres improved mechanical strength, but may also potentially affect cellular activity[33,59,99].

5. Current progress of developing microgels as bioinks in extrusion-based 3D bioprinting

Over the past decade, various 3D bioprinting strategies with distinct characteristics have been developed. Currently, the mainstream strategies include inkjet bioprinting, stereolithography, laser-assisted bioprinting, electrospinning-based bioprinting, and extrusion-based bioprinting[10]. Extrusion-based 3D bioprinting is one of the most common printing methods, mainly due to several advantages of extrusion-based bioprinting over other methods, including (i) the ability to use a variety of bioinks to create tissue structures; (ii) the manufactured structure having physiologically relevant cell density; (iii) the relatively low cell damage during the bioprinting process; (iv) the ability to create scalable structures with anatomically precise geometries; and (v) being relatively low-cost. Its main drawbacks are as follows: (i) it can damage cells during the extrusion process; and (ii) the resolution of the printed product is relatively low and the feature size is limited. The application of microgels is expected to address these issues, and therefore, in this section, we mainly focus on the research progress of microgels in this type of printing strategy[100,101].

Direct bioink writing refers to the direct extrusion of bioinks with rheological properties to form a predetermined shape and configuration at a designated location. During the extrusion process, the bioink behaves like a fluid and then transforms into a solid state upon extrusion[102]. The advantages of direct bioink writing lie in its simplicity and high repeatability. However, when using traditional hydrogels as bioinks, dense gels and/or other components may hinder cell diffusion and migration, and high pressure or shear forces may cause cell damage and/or death[103-105]. Microgels used as bioinks for direct writing can effectively overcome these limitations. The performance of microgels prepared by different preparation and assembly strategies also varies in direct bioink writing.

5.1. Improvement of the geometric structure of microgels

Generally, mechanical fragmentation method involves the physical fragmentation of pre-formed hydrogels to produce microgel. For example, crosslinked hydrogels can be mechanically forced through a fine steel mesh to form smaller microgel, with the size of the microgel being controlled by altering the aperture shape and size of the steel mesh. The main advantages of mechanical fragmentation methods are their speed and simplicity, with the simple process being able to rapidly generate a large amount of micromicrogel. However, the disadvantage is that the shape and size of the generated microgel are difficult to accurately control, which justifies the limited number of reports concerning its performance in 3D bioprinting in the past decades[27].

Flégeau *et al.* reported a microgel suitable for 3D bioprinting made from tyramine-modified hyaluronic acid, which was obtained through mechanical fragmentation and enzymatically crosslinked through the addition of horseradish peroxidase and hydrogen peroxide[96]. The gel was then screened through metal grids with pore sizes of 40, 100, and 500 μm, resulting in a microgel with tyramine residues that could undergo secondary crosslinking to stabilize the scaffold (Figure 4A and B). The product of the secondary crosslinking was found to fully degrade after soaking in hyaluronic acidase for 20 days and demonstrated excellent stability with no swelling in phosphate-buffered saline (PBS) for 21 consecutive days. After sieving, all the microgels displayed shear-thinning behavior, with the yield stress of approximately 139 Pa for microgels of all sizes, which were capable of being printed, but the use of 40 μm-sized microgel resulted in higher-resolution products (Figure 4C). Cells also displayed good viability in microgels produced through mechanical fragmentation, with cell viability at 75.7 ± 8.2%, 73.1 ± 9.4%, and 70.2 ± 9.0% on day 1 for 40, 100, and 500 μm-sized microgel products, respectively, and maintained high viability at 94.5 ± 4.7%, 93.4 ± 1.3%, and 94.1 ± 4.6% on day 21, respectively. The research of Flégeau *et al.* demonstrates that microgels produced through mechanical fragmentation possess good cell compatibility and printing characteristics, and the preparation method is simple and quick[96].

Kessel *et al.* utilized HA-MA as the raw material and constructed a class of entangled microfiber-based large-

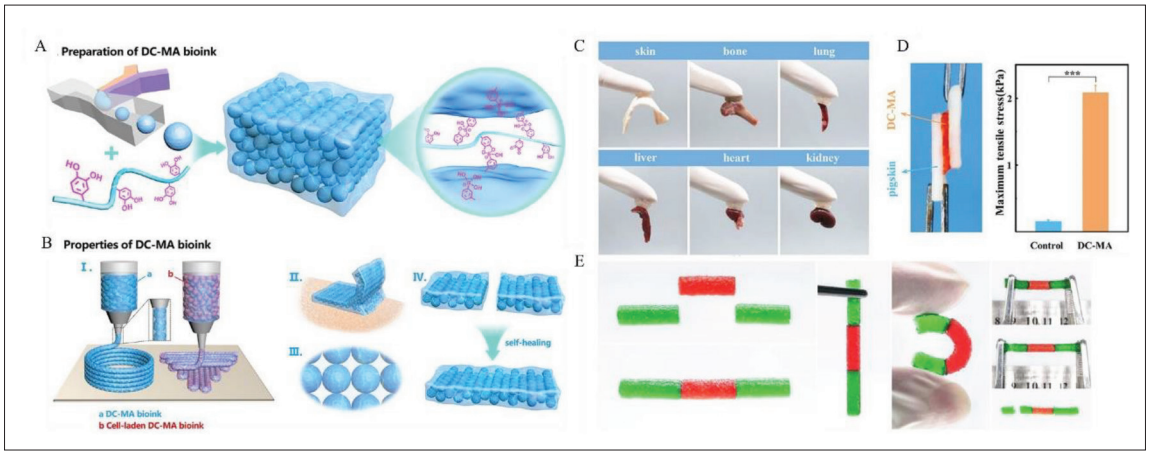

Figure 5. Dynamic crosslinked assembly of microgels as bioinks. (A) Preparation of DC-MA bioink including microfluidic generation of microgels and assembling microgels via dynamic crosslinker. (B) Properties of DC-MA bioink include (I) printability, (II) tissue adhesion, (III) microporosity, and (IV) self-healing. (C) Adhesion of DC-MA to tissues and organs such as pig skin, rabbit bone, mouse lung, mouse liver, mouse heart, and mouse kidney. (D) Maximum tensile stress of pig skins bonded by DC-MA. (E) Self-healing of DC-MA rods. Reprinted with permission from Feng Q, Li D, Li Q, *et al*., 2022, Assembling microgels via dynamic cross-linking reaction improves printability, microporosity, tissue-adhesion, and self-healing of microgel bioink for extrusion bioprinting. *ACS Appl Mater Interfaces*, 14:15653–15666. Copyright 2022 American Chemical Society[113].

pore microgel through mechanical fracture (Figure 4D). First, the HA-MA hydrogel is mechanically fractured through a sieve with a pore size of 40–100 μm. This process deconstructs the hydrogel into microchains, which randomly intertwine with each other to form a high aspect ratio microgel. This type of microgel is more stable than particle-like microgel, and can maintain its shape in aqueous media for 7 days without undergoing secondary crosslinking. Through shear recovery testing, it was found that microgels of various sizes have printability. This strategy was tested by printing a 3D model of a human ear for half of its size. The printed product had a stable structure, and no flowing liquid was observed. Using microgel with a size of 40 μm, cell compatibility was tested, and the results showed that the cell viability before printing, on the 1st day, 7th day, and 21st day were 95.3 ± 0.5%, 90.1 ± 0.6%, 92.3 ± 1.1%, and 92.6 ± 2%, respectively[97].

The use of irregular microgels in bioink formulations can provide several advantages, such as enhanced printability, cell viability, and biofunctionality. Moreover, the complex geometries and tunable mechanical properties of irregular microgels can better mimic the native extracellular matrix (ECM) in various tissues, which could ultimately promote tissue regeneration and repair.

5.2. Improvement of microgel crosslinking methods

Despite the ease of achieving shear-thinning and cell-encapsulating properties using microgels in direct bioink writing, there still exist some issues in the printing process that need to be addressed. For example, due to the microparticulate nature of microgel and their weak intermolecular interactions, microgel bioink is unable to undergo continuous stretching, resulting in relatively thicker and rougher strands upon extrusion[99]. Reducing the size of the microgel and increasing its mechanical modulus can improve its printability and shape fidelity, but this is detrimental to the encapsulation of cells and the maintenance of their viability after encapsulation[67,106]. Additionally, the weak physical interactions between microgel often require a second crosslinking after extrusion in order to enhance the mechanical stability of the printed 3D structure, which can potentially further compromise the viability of cells[26,57,95]. To address this challenge, dynamic hydrogel systems based on external stimuli such as hydrolysis, locally produced enzymes, and light have been developed to regulate degradation[107,108]. The main types of bioinks include dynamic covalent bioinks and supramolecular bioinks[109,110].

One promising solution for enhancing the intermolecular interactions of microgel while still maintaining their shear-thinning properties is the establishment of dynamic covalent bonds between microgel[111,112].When subjected to external force, dynamic covalent bonds are significantly disrupted, giving the microgel-based bioink good shear thinning properties. Upon reduction of external force, the dynamic covalent bonds quickly recover, conferring the microgel-based bioink excellent self-healing properties and mechanical strength. Feng *et al.* prepared a dynamic crosslinked microgel, which was synthesized from the crosslinking of transparent hyaluronic acid (HAMA-PBA) modified with methacrylate and phenyl boronic acid and GelMA through a microfluidic device, and assembled into DC-MA bioink (Figure 5A)[113]. The DC-MA bioink was obtained by adding HA-DA in the microgel, forming

dynamic phenyl boronate bonds between the microgel, which improved the printing properties and shape fidelity of the DC-MA bioink without sacrificing the encapsulated cell viability, and did not require secondary crosslinking to stabilize the printed 3D structure (Figure 5B). According to the experimental data analysis, the storage modulus of the microgel bioplastic ink (325 Pa) is significantly lower than that of the DC-MA bioplastic ink (1926 Pa). The viscosity of the DC-MA bioplastic ink (56,210 Pa·s) at zero shear rate is higher than that of the microgel bioplastic ink (22,650 Pa·s). Additionally, the DC-MA bioplastic ink exhibits stronger adhesion properties, with a maximum viscosity of 83,000 Pa·s compared to the microgel bioplastic ink's maximum viscosity of only 19,000 Pa·s. As a result, this class of microgel readily adheres to tissue and possesses a formidable ability for self-healing (Figure 5C–E)[113].

The extracellular matrix (ECM) is a complex mixture of proteins, polysaccharides, and their combination, which interact through noncovalent interactions to provide temporal and spatial control of the cellular environment and response. Supramolecular bioink utilizes the self-assembly of microgels through the reproduction of such noncovalent interactions. Additionally, supramolecular bioink often has self-healing, shear thinning, stress relaxation, strain hardening, and stimulus response properties[109,114-116].

5.3. Improvement of microgel printing methods

One strategy for 3D bioprinting involves extruding liquid biomaterials in coagulation baths or support baths, which function as coagulation baths to rapidly gel the biomaterials[117]. Coagulation baths typically consist of a liquid that triggers physical or chemical crosslinking of bioink[118,119]. For example, the use of bioink based on alginate for 3D printing involves depositing the bioink in a calcium chloride solution to promote ionic crosslinking of the alginate-containing bioink upon extrusion, resulting in a stable structure. This approach has the advantage of separating the rheological properties of the bioink from its printability, expanding the design freedom of the bioink[120]. However, this strategy has several major drawbacks: (i) coagulation baths can quickly spread within the needles of the print port and block the ink outlet; and (ii) issues related to the adhesion of continuous layers, the buoyancy of deposited fibers, and turbulence generated during the printing process often restrict the overall reproducibility and precision of the printed structure[117,121]. Co-axial wet-spinning can be considered an evolution of the coagulation bath, in which the bioink and crosslinking solution are co-extruded from a single deposition nozzle under laminar flow conditions, ensuring a high degree of reproducibility in the deposition process[101]. However, this technique almost inevitably requires the use of calcium alginate hydrogels or other complex substitute materials, thus presenting certain limitations[117].

To overcome these issues, a new strategy method has recently been proposed, utilizing high-volume-fraction soft microgel or colloids (such as microgel) as the coagulation baths or support baths. Due to the rheological properties of the microgel, they will fluidize at the injection point and then rapidly solidify[122]. Compaan *et al.* prepared microgel of Gellan hydrogel through mechanical breaking method, which resulted in irregular microgel and aggregates with an average diameter of 50 ± 34 μm[123]. Similarly, 5% and 10% agarose were transformed into microgel through transglutaminase crosslinking, resulting in particle diameters of 260 ± 200 μm and 125 ± 100 μm, respectively. These were used as Gellan hydrogel–agarose and agarose–agarose matrices for 3D bioprinting as solidification baths (support baths), with 2% alginate PBS solution used as the extruded ink. The specific printing pattern is shown in Figure 6A. Prior to printing, the support baths were crosslinked and had a total polymer concentration range of 3.5%–13% w/v. A lower concentration of polymer network is beneficial for material exchange while still maintaining mechanical strength, as data from this study showed that the effective stiffness of the composite materials of agarose (3%)–gellan (0.5%), agarose (3%)–agarose (5%), and agarose (3%)–agarose (10%) were 14.9, 14.4, and 36.3 kPa, respectively. The microgel support bath exhibits solid behavior when stationary, but becomes liquid at the injection site during printing and subsequently solidifies to form channels. In addition to creating channels, this strategy allows for the printing of 3D solid objects, as shown in Figure 6B, which can rapidly transform any 3D shape from a computer model into a solid hydrogel object, making complex printing more straightforward[123].

Bhattacharjee *et al.* utilized this microgel-based 3D printing method to construct a variety of interesting and elegant 3D patterns, demonstrating the vast potential of the microgel support bath strategy in 3D bioprinting[124]. They first prepared a microgel medium through crosslinked PVA hydrogel and fluorescent colloids, and utilized an injection head with an inner diameter of 50 μm for writing to create several complex multi-scale structures (Figure 7A)[124]. The metabolic needs of cells require dense vascular systems, which pose a significant challenge for 3D bioprinting[125]. Perhaps, this strategy can be utilized to address this challenge. Dumont *et al.* constructed a complex tubular structure (Figure 7B) with a stable structure that can adjust the thickness of the tube wall (~200 μm) by increasing the writing rate[90]. This microgel-based support bath printing strategy eliminates the influence of surface tension, gravity, and particle diffusion, allowing for the writing of materials with unlimited width[126-128].

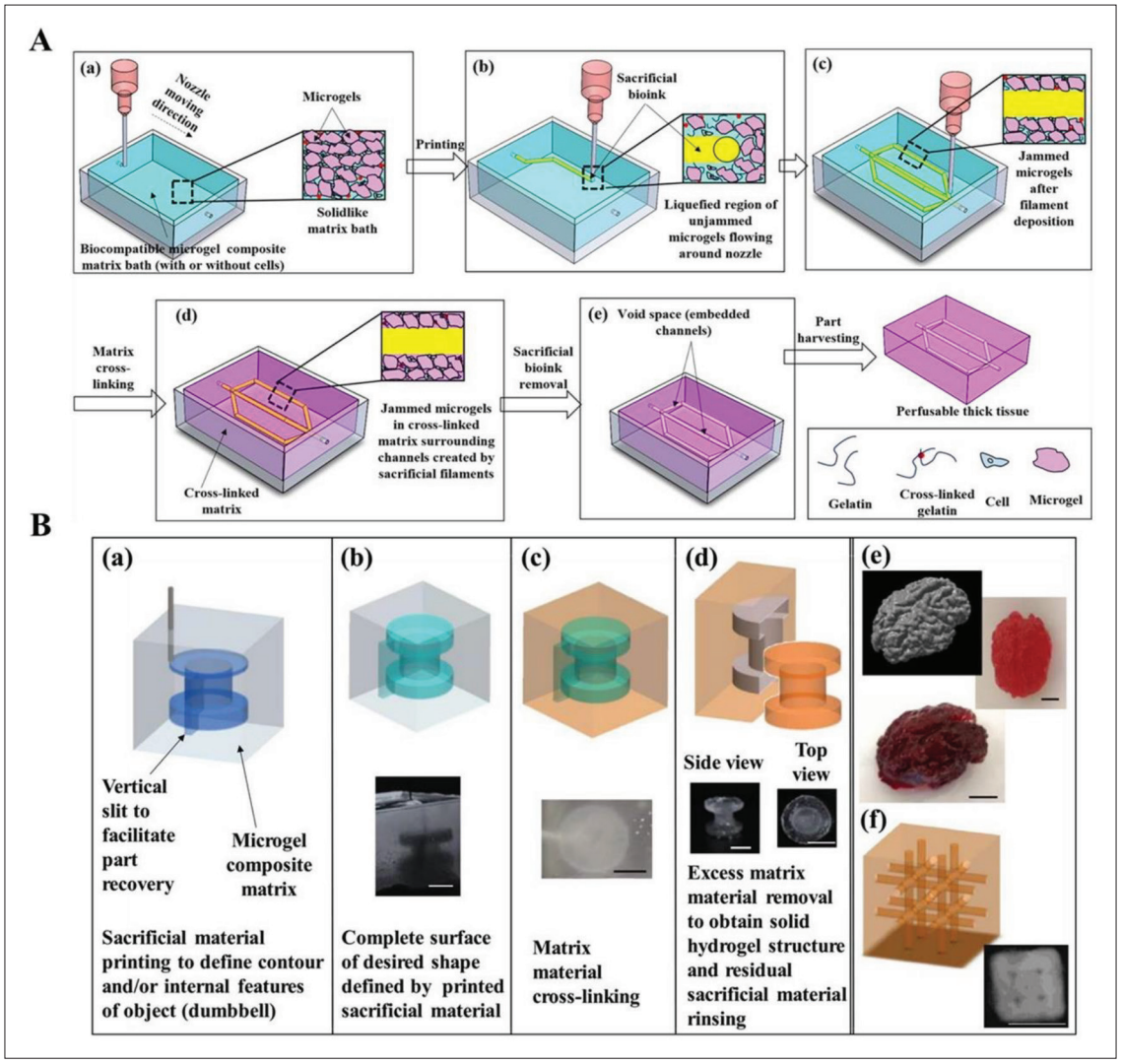

Figure 6. Support bath for 3D printing. (A) Printing schematic showing local behavior of the (a) static and (b) disrupted matrix bath material during printing as well as (c) stabilization of the deposited sacrificial fluid by a solid-like composite hydrogel matrix after printing. After (d) crosslinking, it shows (e) macrostructural and microstructural features of final construct. (B) Embedded surface printing for solid object sculpting: (a) schematic of sacrificial material printing including slit to facilitate part harvesting, (b) complete exterior contour of the dumbbell construct defined by a printed sacrificial material shell, (c) cured hydrogel composite block with embedded object contour, (d) removal of the external composite hydrogel matrix material to recover a solid sculpted hydrogel object; and schematics and photos of other structures fabricated by solid object sculpting: (e) sculpted brain model based on medical imaging data and (f) sculpted lattice block with internal channels[123]. Reprinted with permission Compaan AM, Song K, Chai W, *et al*., 2020, Cross-linkable microgel composite matrix bath for embedded bioprinting of perfusable tissue constructs and sculpting of solid objects. *ACS Appl Mater Interfaces*, 12:7855–7868. Copyright 2020 American Chemical Society[123].

6. Applications of microgels in the field of biomedicine

The continuous development of bioinks has made it possible for 3D bioprinting to transform from concept validation to clinical application. The concept of on-demand bioprinting of tissues (such as blood vessels, nerves, and bone/cartilage) to complete organs has become an ideal solution to addressing the shortage of donor organs for regenerative medicine[10]. Natural tissues are composed of various cells, extracellular matrix, growth factors, and bioactive substances. These diverse components coordinately contribute to the formation of functional tissues or organs[6,129]. The cellular populations of these tissues or organs are closely connected through a unique extracellular matrix, facilitating the exchange of material information such as growth factors, hormones, and other bioactive molecules within the microenvironment in which the cells reside[130,131].

6.1. Bone and cartilage tissue

Various diseases (such as osteoarthritis and rheumatoid arthritis) and trauma can result in damage to cartilage,

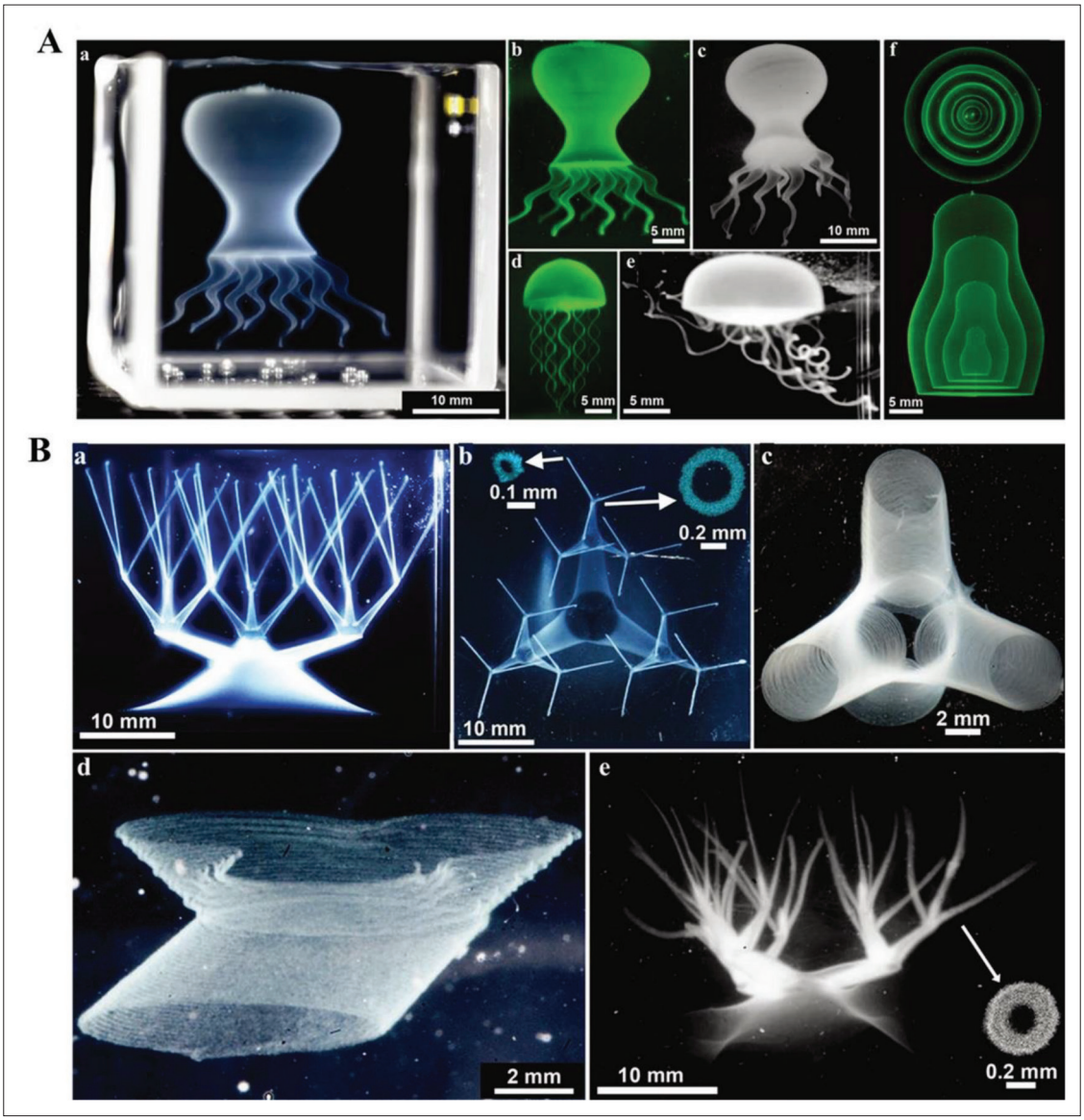

Figure 7. Writing in the granular gel medium. (A) Writing solid shells and capsules. (a) Thin-shell model octopus made from multiple connected hydrogel parts. (b) Octopus model aggregates without structural changes. (c) Octopus model maintains integrity after aggregation. (d) A model jellyfish incorporates flexible high aspect ratio tentacles attached to a closed-shell body. (e) Freely floating in water, the jellyfish model exhibits robustness and flexibility. (f) Model Russian dolls demonstrate the ability to encapsulate with nested thin shells. (B) Hierarchically branched tubular networks. (a, b) A continuous network of hollow vessels with features spanning several orders of magnitude in diameter and aspect ratio. (c) A high-resolution photo of truncated vessels around a junction shows hollow tubes with thin walls and features about 100 μm in diameter. (d) Junctions exhibit stable concave and convex curvatures. (e) Products extracted from granular gels are able to preserve stable structures [from ref.[124] licensed under Attribution-NonCommercial 4.0 International (CC BY-NC 4.0)].

which has a slow rate of regeneration with almost no self-healing ability. Current conventional medications can only alleviate the progression of damage, but cannot cure it. The use of microgel as a bioink for 3D bioprinting of cartilage tissue offers a new strategy for the treatment of cartilage damage[132-134]. Jeon *et al.* designed a light-crosslinked methacrylate oxide algal acid salt (OMA) microgel for printing cartilage and bone tissue, with MSCs able to be loaded onto the OMA microgel. After being frozen and stored for one month, the loaded MSCs retained good biological abilities for cell proliferation and differentiation (osteogenic and chondrogenic differentiation). In addition, the OMA microgel can be printed into various bone tissue shapes (such as femur and skull) in a gelatin support bath[135]. It has been observed that ordinary hydrogels restrict cellular volume expansion, rendering the

cells unable to effectively carry out biological functions. In order to promote cartilage regeneration, Zhu *et al.* developed a microgel composed of hyaluronic acid, PEG, and gelatin that is capable of mixing with cartilage cells and maintaining cellular phenotype, promoting cellular volume expansion and matrix deposition[136]. By injecting the microgel directly into the site of cartilage defects and reinforcing it through photopolymerization, a scaffold is formed to support cartilage regeneration. This microgel has shown promising results in animal experiments, as demonstrated through immunohistochemical staining that revealed an increased presence of *Aggrecan* and COL2 within the interstices of the microgel and a matrix more closely resembling native cartilage[136]. Flégeau *et al.* prepared an enzyme-crosslinked hyaluronic acid microgel through mechanical crushing, which can be used as a bioink for 3D printing to repair cartilage tissue[96]. Its advantage is that the pore size can be adjusted (from 9% to 21%), and the microgel containing human ear cartilage cells can form a stable 3D structure after printing and the printed product can develop stably *in vitro*. GAG, type II collagen, and type I collagen are uniformly and strongly deposited in the gaps between the microgel scaffolds, and the mechanical strength of the printed product can reach approximately 200 kPa after 63 days of *in vitro* cultivation[96]. Chai *et al.* prepared a SilMA/GelMA microgel by mixing low concentrations of GelMA with a certain concentration of methyl methacrylate silk protein (SilMA). The strength of the SilMA/GelMA microgel was greater than that of pure GelMA hydrogel, and it had good biocompatibility, which ensured higher cell survival rates. It also demonstrated good performance in repairing bone defects. In animal experiments, the average bone volume/total volume (BV/TV) at 2 weeks was 6.98% in the rat calvarial defect model repair, which was significantly higher than the average BV/TV (4.56%) in the control group[137].

6.2. Vascularized tissues and structures

The vascular system is crucial for the regeneration of most damaged tissues, as it facilitates the exchange of nutrients, waste, and gases necessary for cell proliferation. Endothelial cells arranged within the vasculature promote healthy blood flow and the exchange of nutrients with surrounding tissues; therefore, the formation of these structures during vascularization is crucial for guiding tissue growth[138-140]. Parthiban *et al.* studied the use of a microgel composed of methylacrylate-functionalized ECM proteins of bone cells for 3D-printing vascularized tissues[141]. This microgel is primarily composed of frozen demineralized and decellularized bone matrix, which maintains the biological advantages associated with the composition of natural ECM and has strong capacity for cell loading and vascular formation. In *in vitro* experiments for vascular generation, the bone matrix microgel group showed significantly better rates, numbers, and lengths of vascular formation compared to the GelMA group. The bone matrix microgel group formed a stable vascular network on the first day, while the GelMA group only formed a relatively stable vascular network on the third day. The number of formations in the bone matrix microgel group was 2.6 times that of the GelMA group, and the length was 6.1 times that of the GelMA group[141].

6.3. Neuronal tissues

The construction of neuronal tissue is made difficult and complex by the presence of various types of cells, electrical conduction, growth factors, and cell orientation[142,143]. The incorporation of ECM-based polymers into ink in combination with cells provides tissue specificity. Kajtez *et al.* developed self-healing, annealing particle-ECM (SHAPE) microgel as a biological ink[144]. SHAPE microgels are composed of a viscous polymer (ECM) solution (continuous phase, approximately 30% volume fraction) and soft water gel (alginate) microgel (discontinuous phase, approximately 70% volume fraction). These microgels provide not only physical support for high-fidelity embedded printing, but also a microenvironment for cellular interaction that supports healthy cellular growth, maturation, and activity[144]. Hsu *et al.* used mechanical disruption to construct a transparent hyaluronic acid microgel loaded with human induced pluripotent stem cell (hiPSC)-derived cortical neurons[145]. The printed product of this microgel was able to support the formation of well-organized neural and astrocytic cell clusters and high levels of axonal extension both within and outside the scaffold. In comparison, the length of axons in the control group was three times shorter than that in the microgel. Furthermore, this microgel scaffold supported long-term culture of neural stem cells, with the cells proliferating and differentiating into large and densely packed clusters of cells after 3 months of cultivation, with the majority being neural cells surrounded by extensively growing axons both within and outside the microgel scaffold, which were well-organized and projecting[145]. Microgels have been demonstrated to simulate ECM structure to promote neural regeneration. Yang *et al.* further validated this conclusion through their study in which they repaired a 10-mm long gap in the sciatic nerve using hyaluronic acid microgel[146].

6.4. Organoids

In addition to being used for printing tissue organs, microgel as a biological ink can also be used to simulate tissue microenvironments, establish organoid models, and reconstruct and simulate *in vitro* 3D environments, providing new approaches for modeling and disease

development. Molley *et al.* directly inscribed the vascular system channels and tumor cell aggregates in a microgel matrix containing cells, creating a tumor microenvironment model[147]. More importantly, this microgel 3D printing approach is almost applicable to all types of cell integration[147].

7. Summary and outlooks

The past decades have seen the rapid progression of 3D bioprinting from concept validation to *in vivo* printing of corresponding structures. However, strategies for 3D bioprinting are still in the exploratory stages of development, with many different strategies being tested, evaluated, refined, and integrated. The full clinical translation of bioprinted tissues and organs is highly challenging and may take a significant amount of time before 3D bioprinting can be fully utilized for organ transplantation or reconstruction of damaged tissues such as blood vessels, nerves, and cartilage. There are still many challenges to be addressed in achieving full clinical translation of 3D bioprinting, but in recent years, microgel have shown great potential as a bioink for 3D bioprinting.

Microgels are a class of novel biomaterials that possess numerous advantageous characteristics. As a bioink, microgel is typically formed by assembling water-based microgel into a 3D printable medium material through various assembly methods[66,148]. The most common method of assembly is achieved through the accumulation of microgel–microgel, which in theory, accumulate randomly to form a microgel with a degree of accumulation known as the accumulation fraction. Microgels with an accumulation fraction greater than 0.58 exhibit a "jamming" state due to the interactions between the microgel–microgel, which grants them unique physical characteristics such as self-assembly, shear thinning, and self-healing. Therefore, microgel in a "jamming" state are highly performing bioinks with micron-level pores for cell loading and maintenance of cell viability, as well as with good shear thinning properties for printing. The "jamming" microgel is essentially a dynamic scaffold, in which the interstitial space between accumulated microgel often forms a 3D, interconnected porous network. Cells can freely migrate through this network and engage in biological information transfer, which is one of the major advantages over traditional hydrogels. The pore size of traditional hydrogels is in the nanometer range, which is not suitable for cell growth and communication.

In addition to the assembly method of gravity-induced accumulation that causes "jamming" of microgel, microgel can also be assembled through other means, such as the assembly of microgel through the interaction of two microgels with opposite charges. The additional interacting forces enhance the mechanical properties and self-healing ability of the microgel. In addition to charge interaction, common mechanisms of interparticle interaction include covalent interaction, adhesive and additive, coordination interaction, and interpenetrating network and other supramolecular interactions. Feng *et al.* utilized dynamic crosslinking to replace the simple accumulation of microparticle microgel, thereby enhancing the porosity, adhesiveness, and self-healing properties of the resulting microparticle gel[28]. Microgels can be assembled through various forms of interparticle interaction forces, and the assembly strategies used can be employed individually or in combination, making the design of microgel more diversified and more adaptable to diverse 3D bioprinting applications.

Porosity is one of the important characteristics of microgel, and multiple studies have found that its porosity not only affects the mechanical properties of microgel, but also affects cell infiltration and migration. Therefore, the optimal porosity of microgel is a focus of concern for many researchers[149]. Seymour *et al.* demonstrated a simple and easy-to-use method for controlling pore size in hydrogels[89]. By crosslinking a mixture of gelatin and GelMA micromicrogel, the pore size of the resulting GelMA hydrogel can be controlled by removing the gelatin micromicrogel. Hydrogels with different pore sizes exhibit different properties[89]. The use of a combination of various types of microgel–microgel to control pore size is a widely utilized strategy, but it has proven difficult to develop a comprehensive theoretical system for guiding the creation of microgel with controllable pore size. In response to this challenge, mathematicians and engineers have studied specific algorithms to calculate and analyze the pore space between stacked microgel, continuously optimizing the algorithms through comparison and analysis of simulated and actual results. While progress has been made, this research offers a new approach for future control of pore size in microgel[150-152]. In addition to studying the preparation of controllable pore size microgel, the preparation of inhomogeneous pore size asymmetrical microgel is also a research direction that deserves our attention. For example, microgel with inhomogeneous and shape-variable pore sizes can be produced through mechanical breaking methods. Using this method, bioinks in special shapes such as "microchains" can be produced, which possess characteristics such as high porosity, large pore size, and high strength, and hold great potential in bone repair[97].

In addition to the conventional use of microgels as bioinks, the 3D bioprinting strategy of using microgels as support baths can also produce products with complex 3D

structures. Simply put, microgels, which are formed from hydrogel–microgel with certain rigidity, are materials that can smoothly transition from solid state to liquid state, and vice versa. Therefore, under the impact of printing injection ports, the microgel liquefies and quickly solidifies after the external force is removed, forming the desired shape. This microgel printing method eliminates the influence of surface tension, gravity, and particle diffusion, enhancing the design freedom of the printed structure. Bhattacharjee *et al.* utilized microgel support baths to print a range of shapes with high aspect ratios, demonstrating the precision and versatility of this method[124]. This type of microgel-based printing strategy is versatile and can be extended to various fields in biomedicine. Compaan *et al.* utilized this strategy to print the fundamental structure of a vascular system, namely well-connected branching channels formed by fork printing paths[123]. Jeon *et al.* employed this strategy to print high-resolution complex 3D structures for the purpose of repairing bone defects or cartilage injuries[153]. Taken together, microgel support baths enable precise and high-resolution printing, providing a new strategy for printing complex organ structures such as vascular and neural tissues.

One aspect of 3D bioprinting that has rapidly developed in recent years is the research on new bioinks. Microgels, as bioinks, are able to replicate specific ECMs while maintaining high cell viability and activity, and induce organ-specific cell behavior. As a new type of bioink, microgel not only have the advantages of common hydrogels, but also make up for their deficiencies, making them more suitable for cell survival and ensuring the performance of biological functions. In addition to maintaining cell viability, microgel can enhance mechanical properties by adjusting the particle size and assembly mode, thus meeting the stability requirements of various organ structures. The complexity of organ structure is also a difficulty in 3D bioprinting. By using a microgel support bath, higher degrees of freedom can be achieved for precise printing, providing an effective solution for printing precise tissue structures. Although the research prospects of microgel as a new type of biological ink are very attractive, many challenges still need to be overcome in order to achieve clinical translation. To achieve ideal 3D bioprinting, it is necessary to recreate the complex structure and biological function of tissues and organs. For example, vascular networks, nervous tissue, and cartilage tissue all have complex structures and functions[125,154,155]. At present, vascularized tissues or independent microvascular network structures can be printed through the use of microgel support baths. There are two difficulties in printing neural tissue: (i) the printing medium must have good cell viability and sufficient pores for nerve cells to extend and communicate; and (ii) it is necessary to print fine structures that can simulate the *in vivo* structure of neural tissue. Microgels have the characteristics to solve the above difficulties, so they have great potential in 3D bioprinting of neural tissue. The regeneration of cartilage tissue is also a focus of 3D bioprinting, as cartilage has limited regenerative capabilities and can be broadly categorized into transparent cartilage, fibrous cartilage, and elastic cartilage, which have structural and physiological differences. Osteoarthritis and rheumatoid arthritis are the most common diseases that lead to damage in joint cartilage, and the number of patients suffering from these conditions is increasing annually[156,157]. Normal joint cartilage is an inhomogeneous layered tissue, and this layering is crucial for maintaining the structure and function of cartilage[158-160]. Thus, the particle heterogeneity of hydrogels and higher printing precision can ideally replicate this layered structure for 3D bioprinting. In summary, the recent progress of hydrogels for 3D bioprinting has been impressive, and it can be anticipated that this field will continue to grow and evolve in the coming years, providing solutions for reconstructing intricate and complex organs and replicating specificity of functional tissues.

The use of microgels in 3D bioprinting is still in the initial stages of exploration, with many different approaches being tested, evaluated, refined, integrated, or abandoned. In this review, we focus on the use of microgels in extrusion-based 3D printing, a technology that we believe offers unique advantages in terms of simplicity, versatility, and performance. The future trend of extrusion-based 3D printing is to print multi-layered, high-precision, biologically functional tissue structures, and to achieve this goal, extrusion-based 3D printing in the form of coagulation and support baths has been proposed in earlier studies, and even further coaxial extrusion systems have been proposed. Despite the limitations related to materials, microgels are perfectly adapted to the support bath system. Therefore, in the future, the extrusion-based 3D printing approach should probably focus on the support bath system of microgels. Second, the development of heterogeneity of microgels is the focus of future development. Based on the complexity of the structure and function of cells, tissues and organs, the interconnection of multiple cells, growth factors and cellular microenvironment should be the focus of 3D bioprinting in future. The availability of a diverse array of microgels enables 3D bioprinting involving multiple cells or growth factors from the bottom up. In addition, microgels with micron-sized pores are more suitable for simulating cellular microenvironment.

Acknowledgments

We are grateful for the support of Life Science Institute of Chongqing Medical University.

Funding

This study was financially supported by the National Natural Science Foundation of China, PRC (U22A20284).

Conflict of interest

The authors declare no conflict of interests.

Author contributions

Conceptualization: Yiting Lei, Chengcheng Du
Supervision: Wei Huang, Yiting Lei
Visualization: Chengcheng Du
Writing – original draft: Chengcheng Du
Writing – review & editing: Wei Huang, Yiting Lei

Ethics approval and consent to participate

Not applicable.

Consent for publication

Not applicable.

Availability of data

Not applicable.

References

1. Mao AS, Mooney DJ, 2015, Regenerative medicine: Current therapies and future directions. *Proc Natl Acad Sci U S A*, 112:14452–14459.

   https://doi.org/10.1073/pnas.1508520112

2. Lin L, Jiang S, Yang J, *et al.*, 2022, Application of 3D-bioprinted nanocellulose and cellulose derivative-based bio-inks in bone and cartilage tissue engineering. *Int J Bioprint*, 9.

   https://doi.org/10.18063/ijb.v9i1.637

3. Malda J, Visser J, Melchels FP, *et al.*, 2013, 25th anniversary article: Engineering hydrogels for biofabrication. *Adv Mater*, 25:5011–5028.

   https://doi.org/10.1002/adma.201302042

4. Zhang YS, Yue K, Aleman J, *et al.*, 2017, 3D bioprinting for tissue and organ fabrication. *Ann Biomed Eng*, 45:148–163.

   https://doi.org/10.1007/s10439-016-1612-8

5. Takagi D, Lin W, Matsumoto T, *et al.*, 2019, High-precision three-dimensional inkjet technology for live cell bioprinting. *Int J Bioprint,* 5.

   https://doi.org/10.18063/ijb.v5i2.208

6. Mandrycky C, Wang Z, Kim K, 2016, 3D bioprinting for engineering complex tissues. *Biotechnol Adv*, 34:422–434.

   https://doi.org/10.1016/j.biotechadv.2015.12.011

7. Murphy SV, Skardal A, Atala A, 2013, Evaluation of hydrogels for bio-printing applications. *J Biomed Mater Res A*, 101:272–284.

   https://doi.org/10.1002/jbm.a.34326

8. Sun D, Chang C, Li S, *et al.*, 2006, Near-field electrospinning. *Nano Lett*, 6:839–842.

   https://doi.org/10.1021/nl0602701

9. Ozbolat IT, Hospodiuk M, 2016, Current advances and future perspectives in extrusion-based bioprinting. *Biomaterials*, 76:321–343.

   https://doi.org/10.1016/j.biomaterials.2015.10.076

10. Heinrich MA, Liu W, Jimenez A, *et al.*, 2019, 3D bioprinting: From benches to translational applications. *Small*, 15: e1805510.

    https://doi.org/10.1002/smll.201805510

11. Raman R, Bhaduri B, Mir M, *et al.*, 2016, High-resolution projection microstereolithography for patterning of neovasculature. *Adv Healthc Mater*, 5:610–619.

    https://doi.org/10.1002/adhm.201500721

12. Gao D, Yao D, Leist SK, *et al.*, 2019, Mechanisms and modeling of electrohydrodynamic phenomena. *Int J Bioprint*, 5.

    https://doi.org/10.18063/ijb.v5i1.166

13. Barner-Kowollik C, Bastmeyer M, Blasco E, *et al.*, 2017, 3D laser micro- and nanoprinting: challenges for chemistry. *Angew Chem Int Ed Engl*, 56:15828–15845.

    https://doi.org/10.1002/anie.201704695

14. Chang CC, Boland ED, Williams SK, *et al.*, 2011, Direct-write bioprinting three-dimensional biohybrid systems for future regenerative therapies. *J Biomed Mater Res B Appl Biomater*, 98:160–170.

    https://doi.org/10.1002/jbm.b.31831

15. Guillotin B, Souquet A, Catros S, *et al.*, 2010, Laser assisted bioprinting of engineered tissue with high cell density and microscale organization. *Biomaterials*, 31:7250–7256.

    https://doi.org/10.1016/j.biomaterials.2010.05.055

16. Castilho M, Feyen D, Flandes-Iparraguirre M, *et al.*, 2017, Melt electrospinning writing of poly-hydroxymethylglycolide-co-ε-caprolactone-based scaffolds for cardiac tissue engineering. *Adv Healthc Mater*, 6.

    https://doi.org/10.1002/adhm.201700311

17. Wu Y, 2021, Electrohydrodynamic jet 3D printing in biomedical applications. *Acta Biomater*, 128:21–41.

    https://doi.org/10.1016/j.actbio.2021.04.036

18. Kiran ASK, Veluru JB, Merum S, *et al.*, 2018, Additive manufacturing technologies: An overview of challenges and perspective of using electrospraying. *Nanocomposites*, 4:190–214.

    https://doi.org/10.1080/20550324.2018.1558499

19. Rastogi P, Kandasubramanian B, 2019, Review of alginate-based hydrogel bioprinting for application in tissue engineering. *Biofabrication*, 11:042001.

https://doi.org/10.1088/1758-5090/ab331e

20. Seoane-Viaño I, Januskaite P, Alvarez-Lorenzo C, *et al.*, 2021, Semi-solid extrusion 3D printing in drug delivery and biomedicine: Personalised solutions for healthcare challenges. *J Control Release*, 332:367–389.

https://doi.org/10.1016/j.jconrel.2021.02.027

21. Zhang B, Cristescu R, Chrisey DB, *et al.*, 2020, Solvent-based extrusion 3D printing for the fabrication of tissue engineering scaffolds. *Int J Bioprint*, 6:211.

https://doi.org/10.18063/ijb.v6i1.211

22. Panwar A, Tan LP, 2016, Current status of bioinks for micro-extrusion-based 3D bioprinting. *Molecules*, 21:685.

https://doi.org/10.3390/molecules21060685

23. Ji S, Guvendiren M, 2017, Recent advances in bioink design for 3D bioprinting of tissues and organs. *Front Bioeng Biotechnol*, 5.

https://www.frontiersin.org/articles/10.3389/fbioe.2017.00023

24. Kyle S, Jessop ZM, Al-Sabah A, *et al.*, 2017, 'Printability' of candidate biomaterials for extrusion based 3D printing: State-of-the-art. *Adv Healthc Mater*, 6:1700264.

https://doi.org/10.1002/adhm.201700264

25. Du C, Huang W, 2022, Progress and prospects of nanocomposite hydrogels in bone tissue engineering. *Nanocomposites*, 8:102–124.

https://doi.org/10.1080/20550324.2022.2076025

26. Yang Y, Jia Y, Yang Q, *et al.*, 2023, Engineering bio-inks for 3D bioprinting cell mechanical microenvironment. *Int J Bioprint,* 9:632.

https://doi.org/10.18063/ijb.v9i1.632

27. Daly AC, Riley L, Segura T, *et al.*, 2020, Hydrogel microparticles for biomedical applications. *Nat Rev Mater*, 5:20–43.

https://doi.org/10.1038/s41578-019-0148-6

28. Feng Q, Li D, Li Q, *et al.*, 2022, Microgel assembly: Fabrication, characteristics and application in tissue engineering and regenerative medicine. *Bioact Mater*, 9:105–119.

https://doi.org/10.1016/j.bioactmat.2021.07.020

29. Xavier JR, Thakur T, Desai P, *et al.*, 2015, Bioactive nanoengineered hydrogels for bone tissue engineering: A growth-factor-free approach. *ACS Nano*, 9:3109–3118.

https://doi.org/10.1021/nn507488s

30. Annabi N, Nichol JW, Zhong X, *et al.*, 2010, Controlling the porosity and microarchitecture of hydrogels for tissue engineering. *Tissue Eng Part B Rev*, 16:371–383.

https://doi.org/10.1089/ten.TEB.2009.0639

31. Butcher AL, Offeddu GS, Oyen ML, 2014, Nanofibrous hydrogel composites as mechanically robust tissue engineering scaffolds. *Trends Biotechnol*, 32:564–570.

https://doi.org/10.1016/j.tibtech.2014.09.001

32. Cheng W, Zhang J, Liu J, *et al.*, 2020, Granular hydrogels for 3D bioprinting applications. *VIEW*, 1:20200060.

https://doi.org/10.1002/VIW.20200060

33. Xin S, Deo KA, Dai J, *et al.*, 2021, Generalizing hydrogel microparticles into a new class of bioinks for extrusion bioprinting. *Sci Adv*, 7:eabk3087.

https://doi.org/10.1126/sciadv.abk3087

34. Adnan MM, Dalod ARM, Balci MH, *et al.*, 2018, In situ synthesis of hybrid inorganic–polymer nanocomposites. *Polymers (Basel)*, 10:1129.

https://doi.org/10.3390/polym10101129

35. Ahlfeld T, Cidonio G, Kilian D, *et al.*, 2017, Development of a clay based bioink for 3D cell printing for skeletal application. *Biofabrication*, 9:034103.

https://doi.org/10.1088/1758-5090/aa7e96

36. Zhang H, Cong Y, Osi AR, *et al.*, 2020, Direct 3D printed biomimetic scaffolds based on hydrogel microparticles for cell spheroid growth. *Adv Funct Mater*, 30:1910573.

https://doi.org/10.1002/adfm.201910573

37. Franco CL, Price J, West JL, 2011, Development and optimization of a dual-photoinitiator, emulsion-based technique for rapid generation of cell-laden hydrogel microspheres. *Acta Biomater*, 7:3267–3276.

https://doi.org/10.1016/j.actbio.2011.06.011

38. Truong N, Lesher-Pérez SC, Kurt E, *et al.*, 2019, Pathways governing polyethylenimine (PEI) polyplex transfection in microporous annealed particle (MAP) scaffolds. *Bioconjug Chem*, 30:476–486.

https://doi.org/10.1021/acs.bioconjchem.8b00696

39. Pittermannová A, Ruberová Z, Zadražil A, *et al.*, 2016, Microfluidic fabrication of composite hydrogel microparticles in the size range of blood cells. *RSC Adv*, 6:103532–103540.

https://doi.org/10.1039/C6RA23003B

40. Nisisako T, Torii T, 2008, Microfluidic large-scale integration on a chip for mass production of monodisperse droplets and particles. *Lab Chip*, 8:287–293.

https://doi.org/10.1039/b713141k

41. Kamperman T, Trikalitis VD, Karperien M, *et al.*, 2018, Ultrahigh-throughput production of monodisperse and multifunctional janus microparticles using in-air microfluidics. *ACS Appl Mater Interfaces*, 10:23433–23438.

https://doi.org/10.1021/acsami.8b05227

42. Chen Z, Lv Z, Zhang Z, *et al.*, 2021, Advanced microfluidic devices for fabricating multi-structural hydrogel microsphere. *Exploration*, 1:20210036.

    https://doi.org/10.1002/EXP.20210036

43. Chung CHY, Cui B, Song R, *et al.*, 2019, Scalable production of monodisperse functional microspheres by multilayer parallelization of high aspect ratio microfluidic channels. *Micromachines (Basel)*, 10:592.

    https://doi.org/10.3390/mi10090592

44. Headen DM, García JR, García AJ, 2018, Parallel droplet microfluidics for high throughput cell encapsulation and synthetic microgel generation. *Microsyst Nanoeng*, 4:1–9.

    https://doi.org/10.1038/micronano.2017.76

45. Mao AS, Shin J-W, Utech S, *et al.*, 2017, Deterministic encapsulation of single cells in thin tunable microgels for niche modeling and therapeutic delivery. *Nat Mater*, 16:236–243.

    https://doi.org/10.1038/nmat4781

46. Schuler F, Schwemmer F, Trotter M, *et al.*, 2015, Centrifugal step emulsification applied for absolute quantification of nucleic acids by digital droplet RPA. *Lab Chip*, 15:2759–2766.

    https://doi.org/10.1039/C5LC00291E

47. Azimi-Boulali J, Madadelahi M, Madou MJ, *et al.*, 2020, Droplet and particle generation on centrifugal microfluidic platforms: A review. *Micromachines*, 11:603.

    https://doi.org/10.3390/mi11060603

48. Kim S, Yim S-G, Chandrasekharan A, *et al.*, 2020, On-site fabrication of injectable 131I-labeled microgels for local radiotherapy. *J Controlled Release*, 322:337–345.

    https://doi.org/10.1016/j.jconrel.2020.03.046

49. Agarwal R, Singh V, Jurney P, *et al.*, 2012, Scalable imprinting of shape-specific polymeric nanocarriers using a release layer of switchable water solubility. *ACS Nano*, 6:2524–2531.

    https://doi.org/10.1021/nn2049152

50. Li M, Mei J, Friend J, *et al.*, 2022, Acousto-photolithography for programmable shape deformation of composite hydrogel sheets. *Small*, 18: e2204288.

    https://doi.org/10.1002/smll.202204288

51. Helgeson ME, Chapin SC, Doyle PS, 2011, Hydrogel microparticles from lithographic processes: Novel materials for fundamental and applied colloid science. *Curr Opin Colloid Interface Sci*, 16:106–117.

    https://doi.org/10.1016/j.cocis.2011.01.005

52. Gramlich WM, Kim IL, Burdick JA, 2013, Synthesis and orthogonal photopatterning of hyaluronic acid hydrogels with thiol-norbornene chemistry. *Biomaterials*, 34:10.1016/j.biomaterials.2013.08.089.

    https://doi.org/10.1016/j.biomaterials.2013.08.089

53. Bahney CS, Lujan TJ, Hsu CW, *et al.*, 2011, Visible light photoinitiation of mesenchymal stem cell-laden bioresponsive hydrogels. *Eur Cell Mater*, 22:43–55.

54. Gansau J, Kelly L, Buckley CT, 2018, Influence of key processing parameters and seeding density effects of microencapsulated chondrocytes fabricated using electrohydrodynamic spraying. *Biofabrication*, 10:035011.

    https://doi.org/10.1088/1758-5090/aacb95

55. Naqvi SM, Vedicherla S, Gansau J, *et al.*, 2016, Living cell factories: Electrosprayed microcapsules and microcarriers for minimally invasive delivery. *Adv Mater*, 28:5662–5671.

    https://doi.org/10.1002/adma.201503598

56. Sinclair A, O'Kelly MB, Bai T, *et al.*, 2018, Self-healing zwitterionic microgels as a versatile platform for malleable cell constructs and injectable therapies. *Adv Mater*, 30: e1803087.

    https://doi.org/10.1002/adma.201803087

57. Hinton TJ, Jallerat Q, Palchesko RN, *et al.*, 2015, Three-dimensional printing of complex biological structures by freeform reversible embedding of suspended hydrogels. *Sci Adv*, 1:e1500758.

    https://doi.org/10.1126/sciadv.1500758

58. Ding A, Jeon O, Cleveland D, *et al.*, 2022, Jammed micro-flake hydrogel for four-dimensional living cell bioprinting. *Adv Mater*, 34: e2109394.

    https://doi.org/10.1002/adma.202109394

59. Xin S, Wyman OM, Alge DL, 2018, Assembly of PEG microgels into porous cell-instructive 3D scaffolds via thiol-ene click chemistry. *Adv Healthc Mater*, 7:e1800160.

    https://doi.org/10.1002/adhm.201800160

60. Riley L, Schirmer L, Segura T, 2019, Granular hydrogels: Emergent properties of jammed hydrogel microparticles and their applications in tissue repair and regeneration. *Curr Opin Biotechnol*, 60:1–8.

    https://doi.org/10.1016/j.copbio.2018.11.001

61. Highley CB, Song KH, Daly AC, *et al.*, 2018, Jammed microgel inks for 3D printing applications. *Adv Sci (Weinh)*, 6:1801076.

    https://doi.org/10.1002/advs.201801076

62. Yang J, Zhang YS, Yue K, *et al.*, 2017, Cell-laden hydrogels for osteochondral and cartilage tissue engineering. *Acta Biomater*, 57:1–25.

    https://doi.org/10.1016/j.actbio.2017.01.036

63. Griffin DR, Weaver WM, Scumpia P, *et al.*, 2015, Accelerated wound healing by injectable microporous gel scaffolds assembled from annealed building blocks. *Nat Mater*, 14:737–744.

    https://doi.org/10.1038/nmat4294

64. Song K, Ren B, Zhai Y, *et al.*, 2021, Effects of transglutaminase cross-linking process on printability of gelatin microgel-gelatin solution composite bioink. *Biofabrication*, 14.

https://doi.org/10.1088/1758-5090/ac3d75

65. Sheikhi A, de Rutte J, Haghniaz R, *et al.*, 2019, Microfluidic-enabled bottom-up hydrogels from annealable naturally-derived protein microbeads. *Biomaterials*, 192:560–568.

https://doi.org/10.1016/j.biomaterials.2018.10.040

66. Caldwell AS, Campbell GT, Shekiro KMT, *et al.*, 2017, Clickable microgel scaffolds as platforms for 3D cell encapsulation. *Adv Healthc Mater*, 6:10.1002/adhm.201700254.

https://doi.org/10.1002/adhm.201700254

67. Xin S, Chimene D, Garza JE, *et al.*, 2019, Clickable PEG hydrogel microspheres as building blocks for 3D bioprinting. *Biomater Sci*, 7:1179–1187.

https://doi.org/10.1039/c8bm01286e

68. Li F, Truong VX, Fisch P, *et al.*, 2018, Cartilage tissue formation through assembly of microgels containing mesenchymal stem cells. *Acta Biomater*, 77:48–62.

https://doi.org/10.1016/j.actbio.2018.07.015

69. Jiang W, Li M, Chen Z, *et al.*, 2016, Cell-laden microfluidic microgels for tissue regeneration. *Lab Chip*, 16:4482–4506.

https://doi.org/10.1039/c6lc01193d

70. Harada A, Kobayashi R, Takashima Y, *et al.*, 2011, Macroscopic self-assembly through molecular recognition. *Nat Chem*, 3:34–37.

https://doi.org/10.1038/nchem.893

71. Hsu R, Chen P, Fang J, *et al.*, 2019, Adaptable microporous hydrogels of propagating NGF-gradient by injectable building blocks for accelerated axonal outgrowth. *Adv Sci (Weinh)*, 6:1900520.

https://doi.org/10.1002/advs.201900520

72. Han YL, Yang Y, Liu S, *et al.*, 2013, Directed self-assembly of microscale hydrogels by electrostatic interaction. *Biofabrication*, 5:035004.

https://doi.org/10.1088/1758-5082/5/3/035004

73. Li CY, Wood DK, Hsu CM, *et al.*, 2011, DNA-templated assembly of droplet-derived PEG microtissues. *Lab Chip*, 11:2967–2975.

https://doi.org/10.1039/c1lc20318e

74. Hu Y, Mao AS, Desai RM, *et al.*, 2017, Controlled self-assembly of alginate microgels by rapidly binding molecule pairs. *Lab Chip*, 17:2481–2490.

https://doi.org/10.1039/c7lc00500h

75. Matsunaga YT, Morimoto Y, Takeuchi S, 2011, Molding cell beads for rapid construction of macroscopic 3D tissue architecture. *Adv Mater*, 23:H90–H94.

https://doi.org/10.1002/adma.201004375

76. Gurkan UA, Tasoglu S, Kavaz D, *et al.*, 2012, Emerging technologies for assembly of microscale hydrogels. *Adv Healthc Mater*, 1:149–158.

https://doi.org/10.1002/adhm.201200011

77. Inamdar NK, Borenstein JT, 2011, Microfluidic cell culture models for tissue engineering. *Curr Opin Biotechnol*, 22:681–689.

https://doi.org/10.1016/j.copbio.2011.05.512

78. Du Y, Lo E, Ali S, *et al.*, 2008, Directed assembly of cell-laden microgels for fabrication of 3D tissue constructs. *Proc Natl Acad Sci U S A*, 105:9522.

https://doi.org/10.1073/pnas.0801866105

79. Zamanian B, Masaeli M, Nichol JW, *et al.*, 2010, Interface-directed self-assembly of cell-laden microgels. *Small*, 6:937–944.

https://doi.org/10.1002/smll.200902326

80. Fernandez JG, Khademhosseini A, 2010, Micro-masonry: Construction of 3D structures by microscale self-assembly. *Adv Mater*, 22:2538–2541.

https://doi.org/10.1002/adma.200903893

81. Xu F, Wu CM, Rengarajan V, *et al.*, 2011, Three-dimensional magnetic assembly of microscale hydrogels. *Adv Mater*, 23:4254–4260.

https://doi.org/10.1002/adma.201101962

82. Tasoglu S, Yu CH, Gungordu HI, *et al.*, 2014, Guided and magnetic self-assembly of tunable magnetoceptive gels. *Nat Commun*, 5:4702.

https://doi.org/10.1038/ncomms5702

83. Xu F, Finley TD, Turkaydin M, *et al.*, 2011, The assembly of cell-encapsulating microscale hydrogels using acoustic waves. *Biomaterials*, 32:7847–7855.

https://doi.org/10.1016/j.biomaterials.2011.07.010

84. Groll J, Burdick JA, Cho D-W, *et al.*, 2018, A definition of bioinks and their distinction from biomaterial inks. *Biofabrication*, 11:013001.

https://doi.org/10.1088/1758-5090/aaec52

85. Parak A, Pradeep P, du Toit LC, *et al.*, 2019, Functionalizing bioinks for 3D bioprinting applications. *Drug Discov Today*, 24:198–205.

https://doi.org/10.1016/j.drudis.2018.09.012

86. Skardal A, 2018, Perspective: "Universal" bioink technology for advancing extrusion bioprinting-based biomanufacturing. *Bioprinting*, 10: e00026.

https://doi.org/10.1016/j.bprint.2018.e00026

87. Le LV, Mohindra P, Fang Q, *et al.*, 2018, Injectable hyaluronic acid based microrods provide local micromechanical

and biochemical cues to attenuate cardiac fibrosis after myocardial infarction. *Biomaterials*, 169:11–21.

https://doi.org/10.1016/j.biomaterials.2018.03.042

88. Sideris E, Griffin DR, Ding Y, *et al.*, 2016, Particle hydrogels based on hyaluronic acid building blocks. ACS *Biomater Sci* Eng, 2:2034–2041.

https://doi.org/10.1021/acsbiomaterials.6b00444

89. Seymour AJ, Shin S, Heilshorn SC, 2021, 3D printing of microgel scaffolds with tunable void fraction to promote cell infiltration. *Adv Healthc Mater*, 10:e2100644.

https://doi.org/10.1002/adhm.202100644

90. Dumont CM, Carlson MA, Munsell MK, *et al.*, 2019, Aligned hydrogel tubes guide regeneration following spinal cord injury. *Acta Biomater*, 86:312–322.

https://doi.org/10.1016/j.actbio.2018.12.052

91. Hu Z, Ma C, Rong X, *et al.*, 2018, Immunomodulatory ECM-like microspheres for accelerated bone regeneration in diabetes mellitus. *ACS Appl Mater Interfaces*, 10:2377–2390.

https://doi.org/10.1021/acsami.7b18458

92. Hoare TR, Kohane DS, 2008, Hydrogels in drug delivery: Progress and challenges. *Polymer*, 49:1993–2007.

https://doi.org/10.1016/j.polymer.2008.01.027

93. Li J, Mooney DJ, 2016, Designing hydrogels for controlled drug delivery. *Nat Rev Mater*, 1:16071.

https://doi.org/10.1038/natrevmats.2016.71

94. Bi D, Zhang J, Chakraborty B, *et al.*, 2011, Jamming by shear. *Nature*, 480:355–358.

https://doi.org/10.1038/nature10667

95. Menut P, Seiffert S, Sprakel J, *et al.*, 2012, Does size matter? Elasticity of compressed suspensions of colloidal- and granular-scale microgels. *Soft Matter*, 8:156–164.

https://doi.org/10.1039/C1SM06355C

96. Flégeau K, Puiggali-Jou A, Zenobi-Wong M, 2022, Cartilage tissue engineering by extrusion bioprinting utilizing porous hyaluronic acid microgel bioinks. *Biofabrication*, 14.

https://doi.org/10.1088/1758-5090/ac6b58

97. Kessel B, Lee M, Bonato A, *et al.*, 2020, 3D bioprinting of macroporous materials based on entangled hydrogel microstrands. *Adv Sci (Weinh)*, 7:2001419.

https://doi.org/10.1002/advs.202001419

98. Zhao D, Liu Y, Liu B, *et al.*, 2021, 3D printing method for tough multifunctional particle-based double-network hydrogels. *ACS Appl Mater Interfaces*, 13:13714–13723.

https://doi.org/10.1021/acsami.1c01413

99. Caliari SR, Vega SL, Kwon M, *et al.*, 2016, Dimensionality and spreading influence MSC YAP/TAZ signaling in hydrogel environments. *Biomaterials*, 103:314–323.

https://doi.org/10.1016/j.biomaterials.2016.06.061

100. Askari M, Naniz MA, Kouhi M, *et al.*, 2021, Recent progress in extrusion 3D bioprinting of hydrogel biomaterials for tissue regeneration: A comprehensive review with focus on advanced fabrication techniques. *Biomater Sci*, 9:535–573.

https://doi.org/10.1039/D0BM00973C

101. Mohan TS, Datta P, Nesaei S, *et al.*, 2022, 3D coaxial bioprinting: Process mechanisms, bioinks and applications. *Prog Biomed Eng*, 4:022003.

https://doi.org/10.1088/2516-1091/ac631c

102. Lee JM, Yeong WY, 2016, Design and printing strategies in 3D bioprinting of cell-hydrogels: A review. *Adv Healthc Mater*, 5:2856–2865.

https://doi.org/10.1002/adhm.201600435

103. Luo Y, Lode A, Gelinsky M, 2013, Direct plotting of three-dimensional hollow fiber scaffolds based on concentrated alginate pastes for tissue engineering. *Adv Healthc Mater*, 2:777–783.

https://doi.org/10.1002/adhm.201200303

104. Hockaday LA, Kang KH, Colangelo NW, *et al.*, 2012, Rapid 3D printing of anatomically accurate and mechanically heterogeneous aortic valve hydrogel scaffolds. *Biofabrication*, 4:035005.

https://doi.org/10.1088/1758-5082/4/3/035005

105. Ouyang L, Yao R, Chen X, *et al.*, 2015, 3D printing of HEK 293FT cell-laden hydrogel into macroporous constructs with high cell viability and normal biological functions. *Biofabrication*, 7:015010.

https://doi.org/10.1088/1758-5090/7/1/015010

106. Feng Q, Gao H, Wen H, *et al.*, 2020, Engineering the cellular mechanical microenvironment to regulate stem cell chondrogenesis: Insights from a microgel model. *Acta Biomater*, 113:393–406.

https://doi.org/10.1016/j.actbio.2020.06.046

107. Kharkar PM, Kiick KL, Kloxin AM, 2015, Design of thiol- and light-sensitive degradable hydrogels using Michael-type addition reactions. *Polym Chem*, 6:5565–5574.

https://doi.org/10.1039/C5PY00750J

108. Madl CM, LeSavage BL, Dewi RE, *et al.*, 2017, Maintenance of neural progenitor cell stemness in 3D hydrogels requires matrix remodelling. *Nat Mater*, 16:1233–1242.

https://doi.org/10.1038/nmat5020

109. Webber MJ, Appel EA, Meijer EW, *et al.*, 2016, Supramolecular biomaterials. *Nat Mater*, 15:13–26.

https://doi.org/10.1038/nmat4474

110. Zhu D, Wang H, Trinh P, *et al.*, 2017, Elastin-like protein-hyaluronic acid (ELP-HA) hydrogels with decoupled mechanical and biochemical cues for cartilage regeneration. *Biomaterials*, 127:132–140.

https://doi.org/10.1016/j.biomaterials.2017.02.010

111. Morgan FLC, Moroni L, Baker MB, 2020, Dynamic bioinks to advance bioprinting. *Adv Healthc Mater*, 9:1901798.

https://doi.org/10.1002/adhm.201901798

112. Tu Y, Chen N, Li C, *et al.*, 2019, Advances in injectable self-healing biomedical hydrogels. *Acta Biomater*, 90:1–20.

https://doi.org/10.1016/j.actbio.2019.03.057

113. Feng Q, Li D, Li Q, *et al.*, 2022, Assembling microgels via dynamic cross-linking reaction improves printability, microporosity, tissue-adhesion, and self-healing of microgel bioink for extrusion bioprinting. *ACS Appl Mater Interfaces*, 14:15653–15666.

https://doi.org/10.1021/acsami.2c01295

114. Daley WP, Peters SB, Larsen M, 2008, Extracellular matrix dynamics in development and regenerative medicine. *J Cell Sci*, 121:255–264.

https://doi.org/10.1242/jcs.006064

115. Goor OJGM, Hendrikse SIS, Dankers PYW, *et al.*, 2017, From supramolecular polymers to multi-component biomaterials. *Chem Soc Rev*, 46:6621–6637.

https://doi.org/10.1039/c7cs00564d

116. Jk M, G O, Vm W, 2014, Extracellular matrix assembly: a multiscale deconstruction. *Nat Rev Mol Cell Biol*, 15:771–785.

https://doi.org/10.1038/nrm3902

117. Costantini M, Colosi C, Święszkowski W, *et al.*, 2018, Co-axial wet-spinning in 3D bioprinting: State of the art and future perspective of microfluidic integration. *Biofabrication*, 11:012001.

https://doi.org/10.1088/1758-5090/aae605

118. Khalil S, Sun W, 2009, Bioprinting endothelial cells with alginate for 3D tissue constructs. *J Biomech Eng*, 131:111002.

https://doi.org/10.1115/1.3128729

119. Rajaram A, Schreyer D, Chen D, 2014, Bioplotting alginate/hyaluronic acid hydrogel scaffolds with structural integrity and preserved schwann cell viability. *3D Print Addit Manuf*, 1:194–203.

https://doi.org/10.1089/3dp.2014.0006

120. Rocca M, Fragasso A, Liu W, *et al.*, 2018, Embedded multimaterial extrusion bioprinting. *SLAS Technol*, 23:154–163.

https://doi.org/10.1177/2472630317742071

121. Cui X, Li J, Hartanto Y, *et al.*, 2020, Advances in extrusion 3D bioprinting: A focus on multicomponent hydrogel-based bioinks. *Adv Healthc Mater*, 9:e1901648.

https://doi.org/10.1002/adhm.201901648

122. Jin Y, Chai W, Huang Y, 2017, Printability study of hydrogel solution extrusion in nanoclay yield-stress bath during printing-then-gelation biofabrication. *Mater Sci Eng C*, 80:313–325.

https://doi.org/10.1016/j.msec.2017.05.144

123. Compaan AM, Song K, Chai W, *et al.*, 2020, Cross-linkable microgel composite matrix bath for embedded bioprinting of perfusable tissue constructs and sculpting of solid objects. *ACS Appl Mater Interfaces*, 12:7855–7868.

https://doi.org/10.1021/acsami.9b15451

124. Bhattacharjee T, Zehnder SM, Rowe KG, *et al.*, 2015, Writing in the granular gel medium. *Sci Adv*, 1:e1500655.

https://doi.org/10.1126/sciadv.1500655

125. Miller JS, Stevens KR, Yang MT, *et al.*, 2012, Rapid casting of patterned vascular networks for perfusable engineered three-dimensional tissues. *Nat Mater*, 11:768–774.

https://doi.org/10.1038/nmat3357

126. Cho EC, Kim J-W, Fernandez-Nieves A, *et al.*, 2008, Highly responsive hydrogel scaffolds formed by three-dimensional organization of microgel nanoparticles. *Nano Lett*, 8:168–172.

https://doi.org/10.1021/nl072346e

127. Debord JD, Eustis S, Debord SB, *et al.*, 2002, Color-tunable colloidal crystals from soft hydrogel nanoparticles. *Adv Mater*, 14:658–662.

https://doi.org/10.1002/1521-4095(20020503)14:9<658::AID-ADMA658>3.0.CO;2-3

128. Dimitriou CJ, Ewoldt RH, McKinley GH, 2013, Describing and prescribing the constitutive response of yield stress fluids using large amplitude oscillatory shear stress (LAOStress). *J Rheol*, 57:27–70.

https://doi.org/10.1122/1.4754023

129. Zhang YS, Xia Y, 2015, Multiple facets for extracellular matrix mimicking in regenerative medicine. *Nanomedicine (Lond)*, 10:689–692.

https://doi.org/10.2217/nnm.15.10

130. Place ES, Evans ND, Stevens MM, 2009, Complexity in biomaterials for tissue engineering. *Nat Mater*, 8:457–470.

https://doi.org/10.1038/nmat2441

131. Rice JJ, Martino MM, De Laporte L, *et al.*, 2013, Engineering the regenerative microenvironment with biomaterials. *Adv Healthc Mater*, 2:57–71.

https://doi.org/10.1002/adhm.201200197

132. Harre U, Schett G, 2017, Cellular and molecular pathways of structural damage in rheumatoid arthritis. *Semin Immunopathol*, 39:355–363.

https://doi.org/10.1007/s00281-017-0634-0

133. Latourte A, Kloppenburg M, Richette P, 2020, Emerging pharmaceutical therapies for osteoarthritis. *Nat Rev Rheumatol*, 16:673–688.

https://doi.org/10.1038/s41584-020-00518-6

134. Jiang Y, 2022, Osteoarthritis year in review 2021: Biology. *Osteoarthr Cartil*, 30:207–215.

https://doi.org/10.1016/j.joca.2021.11.009

135. Jeon O, Bin Lee Y, Hinton TJ, *et al.*, 2019, Cryopreserved cell-laden alginate microgel bioink for 3D bioprinting of living tissues. *Mater Today Chem*, 12:61–70.

https://doi.org/10.1016/j.mtchem.2018.11.009

136. Zhu Y, Sun Y, Rui B, *et al.*, 2022, A photoannealed granular hydrogel facilitating hyaline cartilage regeneration via improving chondrogenic phenotype. *ACS Appl Mater Interfaces*, 14:40674–40687.

https://doi.org/10.1021/acsami.2c11956

137. Chai N, Zhang J, Zhang Q, *et al.*, 2021, Construction of 3D printed constructs based on microfluidic microgel for bone regeneration. *Compos Part B Eng*, 223:109100.

https://doi.org/10.1016/j.compositesb.2021.109100

138. Díaz del Moral S, Barrena S, Muñoz-Chápuli R, *et al.*, 2020, Embryonic circulating endothelial progenitor cells. *Angiogenesis*, 23:531–541.

https://doi.org/10.1007/s10456-020-09732-y

139. Filipowska J, Tomaszewski KA, Niedźwiedzki Ł, *et al.*, 2017, The role of vasculature in bone development, regeneration and proper systemic functioning. *Angiogenesis*, 20:291–302.

https://doi.org/10.1007/s10456-017-9541-1

140. Latacz E, Caspani E, Barnhill R, *et al.*, 2020, Pathological features of vessel co-option versus sprouting angiogenesis. *Angiogenesis*, 23:43–54.

https://doi.org/10.1007/s10456-019-09690-0

141. Parthiban SP, Athirasala A, Tahayeri A, *et al.*, 2021, BoneMA-synthesis and characterization of a methacrylated bone-derived hydrogel for bioprinting of in-vitro vascularized tissue constructs. *Biofabrication*, 13.

https://doi.org/10.1088/1758-5090/abb11f

142. Sousa AMM, Meyer KA, Santpere G, *et al.*, 2017, Evolution of the human nervous system function, structure, and development. *Cell*, 170:226–247.

https://doi.org/10.1016/j.cell.2017.06.036

143. Varadarajan SG, Hunyara JL, Hamilton NR, *et al.*, 2022, Central nervous system regeneration. *Cell*, 185:77–94.

https://doi.org/10.1016/j.cell.2021.10.029

144. Kajtez J, Wesseler MF, Birtele M, *et al.*, 2022, Embedded 3D printing in self-healing annealable composites for precise patterning of functionally mature human neural constructs. *Adv Sci (Weinh)*, 9:2201392.

https://doi.org/10.1002/advs.202201392

145. Hsu C-C, George JH, Waller S, *et al.*, 2021, Increased connectivity of hiPSC-derived neural networks in multiphase granular hydrogel scaffolds. *Bioact Mater*, 9:358–372.

https://doi.org/10.1016/j.bioactmat.2021.07.008

146. Yang J, Hsu C-C, Cao T-T, *et al.*, 2023, A hyaluronic acid granular hydrogel nerve guidance conduit promotes regeneration and functional recovery of injured sciatic nerves in rats. *Neural Regen Res*, 18:657–663.

https://doi.org/10.4103/1673-5374.350212

147. Molley TG, Jalandhra GK, Nemec SR, *et al.*, 2021, Heterotypic tumor models through freeform printing into photostabilized granular microgels. *Biomater Sci*, 9:4496–4509.

https://doi.org/10.1039/d1bm00574j

148. Zeng Y, Zhu L, Han Q, *et al.*, 2015, Preformed gelatin microcryogels as injectable cell carriers for enhanced skin wound healing. *Acta Biomater*, 25:291–303.

https://doi.org/10.1016/j.actbio.2015.07.042

149. Brodu N, Dijksman JA, Behringer RP, 2015, Spanning the scales of granular materials through microscopic force imaging. *Nat Commun*, 6:6361.

https://doi.org/10.1038/ncomms7361

150. Roozbahani MM, Borela R, Frost JD, 2017, Pore size distribution in granular material microstructure. *Materials (Basel)*, 10:1237.

https://doi.org/10.3390/ma10111237

151. Jones AC, Arns CH, Hutmacher DW, *et al.*, 2009, The correlation of pore morphology, interconnectivity and physical properties of 3D ceramic scaffolds with bone ingrowth. *Biomaterials*, 30:1440–1451.

https://doi.org/10.1016/j.biomaterials.2008.10.056

152. Schaller FM, Kapfer SC, Hilton JE, *et al.*, 2015, Non-universal Voronoi cell shapes in amorphous ellipsoid packs. *EPL*, 111:24002.

https://doi.org/10.1209/0295-5075/111/24002

153. Jeon O, Lee YB, Jeong H, *et al.*, 2019, Individual cell-only bioink and photocurable supporting medium for 3D printing and generation of engineered tissues with complex geometries. *Mater Horiz*, 6:1625–1631.

https://doi.org/10.1039/c9mh00375d

154. Kolesky DB, Truby RL, Gladman AS, *et al.*, 2014, 3D bioprinting of vascularized, heterogeneous cell-laden tissue constructs. *Adv Mater*, 26:3124–3130.

https://doi.org/10.1002/adma.201305506

155. Bertassoni LE, Cecconi M, Manoharan V, *et al.*, 2014, Hydrogel bioprinted microchannel networks for vascularization of tissue engineering constructs. *Lab Chip*, 14:2202–2211.

https://doi.org/10.1039/c4lc00030g

156. Hunter DJ, Bierma-Zeinstra S, 2019, Osteoarthritis. *Lancet*, 393:1745–1759.

https://doi.org/10.1016/S0140-6736(19)30417-9

157. Weyand CM, Goronzy JJ, 2021, The immunology of rheumatoid arthritis. *Nat Immunol*, 22:10–18.

https://doi.org/10.1038/s41590-020-00816-x

158. Armiento AR, Stoddart MJ, Alini M, *et al.*, 2018, Biomaterials for articular cartilage tissue engineering: Learning from biology. *Acta Biomater*, 65:1–20.

https://doi.org/10.1016/j.actbio.2017.11.021

159. Chijimatsu R, Saito T, 2019, Mechanisms of synovial joint and articular cartilage development. *Cell Mol Life Sci*, 76(20):3939–3952.

https://doi.org/10.1007/s00018-019-03191-5

160. Hodgkinson T, Kelly DC, Curtin CM, *et al.*, 2022, Mechanosignalling in cartilage: An emerging target for the treatment of osteoarthritis. *Nat Rev Rheumatol*, 18:67–84.

https://doi.org/10.1038/s41584-021-00724-w

161. Stenekes RJ, Franssen O, van Bommel EM, *et al.*, 1998, The preparation of dextran microspheres in an all-aqueous system: Effect of the formulation parameters on particle characteristics. *Pharm Res*, 15:557–561.

https://doi.org/10.1023/a:1011925709873

162. Xu Q, Hashimoto M, Dang TT, *et al.*, 2009, Preparation of monodisperse biodegradable polymer microparticles using a microfluidic flow-focusing device for controlled drug delivery. *Small*, 5:1575–1581.

https://doi.org/10.1002/smll.200801855

163. Bardin D, Kendall MR, Dayton PA, *et al.*, 2013, Parallel generation of uniform fine droplets at hundreds of kilohertz in a flow-focusing module. *Biomicrofluidics*, 7:34112.

https://doi.org/10.1063/1.4811276

164. Rolland JP, Maynor BW, Euliss LE, *et al.*, 2005, Direct fabrication and harvesting of monodisperse, shape-specific nanobiomaterials. *J Am Chem Soc*, 127:10096–10100.

https://doi.org/10.1021/ja051977c

165. Pregibon DC, Toner M, Doyle PS, 2007, Multifunctional encoded particles for high-throughput biomolecule analysis. *Science*, 315:1393–1396.

https://doi.org/10.1126/science.1134929

166. Pancholi K, Ahras N, Stride E, *et al.*, 2009, Novel electrohydrodynamic preparation of porous chitosan particles for drug delivery. *J Mater Sci Mater Med*, 20: 917–923.

https://doi.org/10.1007/s10856-008-3638-4

167. Qayyum AS, Jain E, Kolar G, *et al.*, 2017, Design of electrohydrodynamic sprayed polyethylene glycol hydrogel microspheres for cell encapsulation. *Biofabrication*, 9:025019.

https://doi.org/10.1088/1758-5090/aa703c